Geochimica et Cosmochimica Acta Vol. 51, pp. 3087–3103
© Pergamon Journals Ltd. 1987. Printed in U.S.A.
0016-7037/87/$3.00 + .00

Heat capacity measurements for cryolite (Na_3AlF_6) and reactions in the system Na-Fe-Al-Si-O-F*

LAWRENCE M. ANOVITZ[1,4], BRUCE S. HEMINGWAY[2], EDGAR F. WESTRUM, JR.[3], GUY W. METZ[1] and ERIC J. ESSENE[1]

[1]Department of Geological Sciences, Univ. of Michigan, Ann Arbor, MI 48109, U.S.A.
[2]U.S. Geological Survey, 959 National Center, Reston, VA 22092, U.S.A.
[3]Department of Chemistry, Univ. of Michigan, Ann Arbor, MI 48109, U.S.A.
[4]Now at: Department of Geosciences, Univ. of Arizona, Tucson, AZ 85721, U.S.A.

(*Received December* 9, 1985; *accepted in revised form August* 25, 1987)

Abstract—The heat capacity of cryolite (Na_3AlF_6) has been measured from 7 to 1000 K by low-temperature adiabatic and high-temperature differential scanning calorimetry. Low-temperature data were obtained on material from the same hand specimen in the calorimetric laboratories of the University of Michigan and U.S. Geological Survey. The results obtained are in good agreement, and yield average values for the entropy of cryolite of:

$$S^0_{298} = 238.5 \text{ J/mol K}$$

$$S^0_T - S^0_{298} = 145.114 \ln T + 193.009 * 10^{-3} T - 10.366 * 10^5 / T^2 - 872.89 \text{ J/mol K (273–836.5 K)}$$

$$\Delta S_{Trans} = 9.9 \text{ J/mol K}$$

$$S^0_T - S^0_{298} = 198.414 \ln T + 73.203 * 10^{-3} T - 63.814 * 10^5 / T^2 - 1113.11 \text{ J/mol K (836.5–1153 K)}$$

with the transition temperature between α- and β-cryolite taken at 836.5 K.

These data have been combined with data in the literature to calculate phase equilibria for the system Na-Fe-Al-Si-O-F. The resultant phase diagrams allow constraints to be placed on the fO_2, fF_2, $aSiO_2$ and T conditions of formation for assemblages in alkalic rocks. A sample application suggests that $\log fO_2$ is approximately −19.2, $\log fF_2$ is −31.9 to −33.2, and $aSiO_2$ is −1.06 at assumed P/T conditions of 1000 K, 1 bar for the villiaumite-bearing Ilimaussaq intrusion in southwestern Greenland.

INTRODUCTION

CRYOLITE (Na_3AlF_6) is a relatively rare mineral of great importance to the aluminum industry. While Ivigtut, Greenland is perhaps the best known cryolite locality, BAILEY (1980) lists 21 occurrences of cryolite worldwide. Despite its importance, however, the values for the thermodynamic parameters of cryolite are uncertain.

Discordant calorimetric enthalpy values for cryolite are given by ALBRIGHT (1956), O'BRIEN and KELLEY (1957), and HOLM and GRØNVOLD (1973). FRANK (1961) suggested that the temperature scale used by O'Brien and Kelley was in error and corrected the experimental enthalpy values for that error. However, DOUGLAS and DITMARS (1967) suggested that the corrections made by Frank were invalid. STULL and PROPHET (1971), ROBIE *et al.* (1979) and CHASE *et al.* (1985) attempted to reconcile the discordance in the experimental data for the transitions and temperatures of transitions in their tabulations of the thermodynamic data for cryolite, but they left the enthalpy values of O'Brien and Kelley substantially unchanged. Therefore, the enthalpy data used to derive the thermodynamic data for cryolite in the common reference sources for geochemists (STULL and PROPHET, 1971; ROBIE *et al.*, 1979) are inconsistent with data derived from other experimental procedures (*e.g.*, LANDON and UBBELOHDE, 1957). Resolution of this discrepancy is important both for the aluminum industry and for geochemists who are interested in problems involving fluorine-rich granites and hydrothermal systems.

We have measured the heat capacity of a natural sample of cryolite from Ivigtut, Greenland using two adiabatic calorimeters between 5 and 350 K and a differential scanning calorimeter (DSC) between 340 and 1000 K. These results are used to resolve the discordant enthalpy data, to provide revised values of the thermophysical constants for cryolite, and to calculate phase equilibria appropriate to cryolite deposits and nepheline-bearing gneisses.

SAMPLE DESCRIPTION

The sample consisted of a single block of pure cryolite from Ivigtut, Greenland approximately 11 × 4 × 4 cm in size, obtained from the mineralogical collections of the Department of Geological Sciences at the University of Michigan. Examination of the specimen in thin-section showed that the material was complexly twinned but revealed no other mineral phases. Abundant fluid inclusions, however, were found. Scanning electron microscope (SEM) studies of these inclusions showed that some contain crystals of chiolite ($Na_5Al_3F_{14}$). These crystals are too small, and too few in number for their effects on the measured heat capacity to be significant, but the effect of the fluid had to be considered.

* Contribution No. 440 of the Mineralogical Laboratory, Department of Geological Sciences, and the Department of Chemistry, The University of Michigan.

Attempts were made to analyze the sample using the ARL-EMX electron microprobe at the University of Michigan. Unfortunately, even at accelerating voltages as low as 7 kV and sample currents of 2 nA the sample was found to volatilize under the beam. Examination of the energy dispersive (EDA) spectrum, however, revealed only the presence of Na, Al, and F.

For cryogenic measurements at the University of Michigan a single 39.5402 g block of cryolite was slotted to provide a recess for the off-center heating well of the calorimeter. For measurements at the U.S. Geological Survey, however, a block of cryolite was lightly crushed, and material less than 105 microns was removed. The sample contained particles that ranged upward to about 0.125 cm^3. The bulk of the sample mass was contained in particles larger than 1480 microns. The sample (38.5071 g) was loaded into the calorimeter, which was then evacuated. The combined processes of crushing and pumping a vacuum on the sample helped remove some of the water from the fluid inclusions contained in the original block of cryolite.

EXPERIMENTAL METHODS

Low-temperature adiabatic calorimetry was performed on our cryolite sample in two separate calorimeters, one in E. F. Westrum, Jr.'s laboratory at the University of Michigan (UM), and one in R. A. Robie and B. S. Hemingway's laboratory at the U.S. Geological Survey (USGS) in Reston, Virgina, allowing an interlaboratory comparison to be made. All measurements of temperature, time, potential, resistance, and mass are referred to calibrations or standards of the National Bureau of Standards. The USGS uses the IPTS-68 temperature scale and the University of Michigan uses the IPTS-48 scale.

Measurements at the UM were made in the Mark II calorimetric cryostat using a capsule-type resistance thermometer (laboratory designation A-5) and a gold-plated, oxygen-free, high conductivity (OFHC) copper calorimeter (laboratory designation W-61). The general nature of the cryostat and the use of the quasi-adiabatic technique have been described elsewhere (WESTRUM, 1984; WESTRUM *et al.*, 1968).

Low-temperature heat capacity measurements were made at the USGS using the intermittent heating method under quasi-adiabatic conditions (ROBIE and HEMINGWAY, 1972), and using the fully automated calorimeter described by HEMINGWAY *et al.* (1984). The gold plated OFHC copper calorimeter was sealed with a metal O-ring (ROBIE *et al.*, 1976) under pure helium gas at a pressure of 5 kPa. The heat capacity of the sample was 41 percent of the total at 10 K, 50 percent at 50 K, 51 percent at 100 K, 56 percent at 200 K, 58 percent at 300 K, and 58 percent at 375 K.

The high-temperature heat capacity of cryolite was measured between 340 and 1000 K at the USGS using the differential scanning calorimeter (DSC) apparatus and procedures described by HEMINGWAY *et al.* (1981). Temperatures were calibrated against the NBS-ICTA standard reference materials 758 and 759 using 844 K for the α-β transition in quartz and 427 K for the melting point of indium metal (extrapolated onset temperature, see MCADIE *et al.*, 1972). The sample weighed 42.822 mg. One large chip (2 × 4 × 3 mm) and several smaller chips comprised the sample.

EXPERIMENTAL RESULTS

Low-temperature adiabatic results

The experimental low-temperature heat capacity values from both laboratories are presented in order of measurement in Tables 1 and 2. These data are given in terms of joules, an ice point of 273.15 K, and a gram formula weight for cryolite of 209.9413 g. A small adjustment for curvature (<0.1 percent) has been made in some regions for the difference between $C_p = (dH/dT)_p$ and the experimental values of $\Delta H/\Delta T$ based on finite temperature increments, which can usually be inferred from the tabulated adjacent mean temperatures.

In the USGS sample, a thermal anomaly, arising from the melting of fluid inclusions, was first observed in the heat-capacity calculated for cryolite at 271.04 K. A repeat series (Series 4, Table 2) of heat capacity measurements was made with a small temperature increment (about 0.5 K) between 268 and 271 K. The small anomaly was centered near 268.2 K. The amount of water present was estimated as $1.3 * 10^{-4}$ g of water per gram of cryolite from the excess heat capacity and the enthalpy of fusion of water taken from ROBIE *et al.* (1979). This quantity of water would contribute 0.03% excess entropy to the entropy of cryolite at 298.15 K with no correction for the enthalpy of fusion of pure water, or 0.02% when the data were smoothed through the small thermal fusion anomaly as was the practice in this study. No further corrections were made for the fluid inclusions because the error arising from the contributions is an order of magnitude less than the uncertainty of 0.3% in the entropy of cryolite at 298.15 K. The same phenomenon was observed in the UM sample, but a greater fraction of the original fluid inclusions was retained because a massive block sample was used. Calculations suggested that the UM sample contained $3.0 * 10^{-4}$ g of water per gram of sample. Corrections were therefore applied to the measured heat capacity of cryolite for the heat capacity of ice below the melting transition and of water above it.

The smoothed, corrected heat capacity values obtained by integrating the UM data are given in Table 3. These values were taken from a smooth curve obtained by using least-squares methods to fit polynomial functions through the experimental data and extrapolating below 6 K using the Debye limiting law.

The USGS experimental heat capacities were smoothed using the cubic spline procedures described by ROBIE *et al.* (1982). The results are given in Table 3. The experimental results for temperatures below 30 K were plotted as C_p/T *vs.* T^2 and extrapolated smoothly to 0 K. The results for temperatures between 20 and 30 K were smoothly joined with the results of the spline function. The graphical data were manually integrated to 25 K. The spline function was integrated from 25 to 350 K.

These values are estimated to have a probable error of 0.08% above 25 K, and 1% at 12 K, which increases to approximately 6% at 5 K. The thermodynamic functions are considered to have a probable error of less than 0.1% between 100 and 350 K. Additional digits beyond those significant are given in Table 3 for internal consistency and to permit interpolation and differentiation. The entropies and Gibbs energies have not been adjusted for contributions from nuclear spin and isotope mixing and hence are practical values for use in chemical thermodynamic calculations.

The two new sets of cryogenic data reported in this

Table 1: Experimental low-temperature heat capacity determinations on cryolite. University of Michigan values.

T	C_p	T	C_p	T	C_p	T	C_p
K	J/(mol K)	K	J/(mol K)	K	J/(mol K)	K	J/(mol K)
Series I		55.17	44.07	259.50	205.5	273.55	209.6
		57.67	47.43	264.65	207.9	273.88	209.6
6.87	0.1580	60.29	51.01	269.77	213.2	274.20	209.8
8.20	0.1995	63.20	54.98	274.93	211.3		
8.97	0.2411	66.26	59.05	280.20	212.1	Series III	
9.52	0.2503	69.48	63.21	285.94	214.3		
9.99	0.2594	72.86	67.43	292.14	215.7	265.28	208.0
10.46	0.3084	76.10	71.77	298.33	217.8	265.61	207.1
10.96	0.3517	83.74	81.52	304.53	219.3	265.94	206.5
11.45	0.4265	87.85	85.05	310.73	221.0	266.26	207.8
11.96	0.5022	92.17	91.64	316.93	222.7	266.59	209.8
12.50	0.6078	96.73	96.83	323.13	224.4	266.91	208.1
13.06	0.7208	101.54	102.1	329.34	225.9	267.24	208.0
13.64	0.8663	106.50	107.4	335.02	227.1	267.57	210.4
14.25	1.038	111.48	112.6	340.20	228.3	267.89	210.1
14.88	1.252	116.47	117.7	345.37	229.5	268.22	208.9
15.54	1.487	121.48	122.7			268.54	209.3
16.23	1.772	126.50	127.5	Series II		268.87	209.7
16.95	2.099	131.55	132.1			269.19	210.7
17.72	2.463	136.60	136.6	265.40	209.9	269.52	210.3
18.51	2.911	141.65	140.8	265.72	207.4	269.84	212.2
19.34	3.380	145.71	144.9	266.06	207.1	270.16	211.2
20.20	3.930	151.79	149.0	266.39	208.3	270.49	213.2
21.11	4.554	156.86	152.8	266.71	208.3	270.81	213.2
23.11	6.040	161.95	156.6	267.04	207.9	271.13	213.8
24.21	7.004	167.05	160.0	267.36	210.3	271.44	214.2
25.31	7.971	172.15	163.4	267.70	210.8	271.77	213.9
26.47	9.021	177.26	166.5	268.02	210.2	272.09	213.7
27.69	10.22	182.37	169.7	268.35	205.3	272.41	213.7
28.96	11.50	187.49	172.9	268.67	207.0	272.90	210.8
30.30	12.90	192.61	175.8	269.00	206.9	273.05	210.4
31.71	14.44	197.74	178.7	269.32	208.9	273.38	210.0
33.18	16.09	202.88	181.2	269.65	208.7	273.70	210.2
34.73	17.89	208.01	183.9	269.97	208.9	274.02	210.9
36.35	19.81	213.15	186.4	270.30	209.3	274.35	209.9
38.05	21.92	218.29	188.7	270.63	208.8	274.67	210.9
39.85	24.08	223.43	191.1	270.95	209.4	274.99	209.7
41.70	26.43	228.58	193.5	271.28	209.6		
43.70	28.96	233.72	195.6	271.60	210.8		
45.78	31.64	238.87	197.7	272.26	214.5		
47.96	34.52	244.03	199.9	272.58	211.6		
50.25	37.57	249.18	201.8	272.90	210.7		
52.65	40.77	254.34	203.6	273.23	209.4		

paper and the earlier U.S. Bureau of Mines (USBM) data are compared in Table 3. It is evident that the data agree within the combined experimental uncertainties over most of the temperature range. The agreement is somewhat poorer at lower temperatures as expected because of the use of different temperature scales. The agreement between both data sets and the earlier USBM data is also poorer at the lower limit of the USBM data set. Derived thermodynamic functions, in particular the entropy values (*cf.* Table 7) are nevertheless well within the estimated error limits for all three sets of data.

Superambient (DSC) results

The experiment high-temperature specific heats for cryolite are listed in Table 4, and smoothed values for the thermodynamic functions are given in Table 5. Each series represents a continuous scan or experimental setup. Series 7 and 12 were taken at 5 K/min. and at 1.25 K/min., respectively, to better delineate the α-β transition in cryolite observed at 836.5 K. Our results compare favorably with the enthalpy data of O'BRIEN and KELLEY (1957), which were selected by STULL and PROPHET (1971), ROBIE *et al.* (1979) and CHASE *et al.* (1985) in their evaluations of the thermodynamic data for cryolite. Other results are summarized by KELLEY (1960).

STULL and PROPHET (1971) summarized the temperatures reported for the α-β transition in cryolite and selected 838 K at the transition temperature. Our value (836.5) is in good agreement with the findings of LANDON and UBBELOHDE (1957), MAJUMDAR and ROY (1965), ROTH and BERTRAM (1979) and CHASE *et al.* (1985).

Our experimental specific-heat data were fit to equations of the type suggested by HAAS and FISHER (1976). Specific heats below the α-β transition were fit by Eqn. (1):

$$C_p = 17.231 - 1.6236 * 10^{-2}T + 8.4396 * 10^{-6}T^2 - 237.00T^{-0.5} + 1.4331 * 10^{5}T^{-2} \quad (280 \text{ to } 836.5 \text{ K}) \tag{1}$$

with an average deviation of 0.6%. For data taken above the α-β transition, Eqn. (2)

$$C_p = 1.1274 + 2.2857 * 10^{-4}T \quad (836.5 \text{ to } 1000 \text{ K}) \tag{2}$$

Table 2. Experimental low temperature heat-capacity derminations on cryolite. U.S. Geological Survey values.

T	C_p	T	C_p	T	C_p
K	J/(mol K)	K	J/(mol K)	K	J/(mol K)
Series I		Series II		Series IV	
301.47	217.7	141.12	140.3	268.24	238.6
306.03	219.0	146.29	144.5	268.69	209.7
311.00	220.1	151.44	148.5	269.10	209.4
316.02	221.2	156.58	152.4	269.53	209.2
321.21	226.6	161.69	156.1	269.99	208.1
326.40	224.3	166.78	159.6	270.47	208.2
331.58	225.3	171.85	162.9	270.94	209.2
336.75	226.2	176.91	166.1		
341.91	227.2			Series V	
347.06	228.5	Series III			
352.20	229.5			298.64	217.1
357.79	230.6	182.02	169.5	302.96	218.5
363.86	231.7	187.25	172.6	307.90	219.4
369.94	232.8	192.39	175.4		
376.00	234.1	197.54	178.1	Series VI	
		202.89	181.0		
Series II		208.25	183.7	8.09	0.0977
		213.60	186.3	8.77	0.1383
46.48	32.09	218.93	188.8	9.77	0.2271
51.28	38.28	224.26	191.2	10.90	0.3511
55.45	43.86	229.62	193.4	12.07	0.5295
60.53	50.69	235.01	195.7	13.40	0.8137
66.67	58.98	240.41	198.1	14.86	1.233
72.73	67.13	250.68	201.8	16.46	1.847
78.90	75.30	255.48	203.6	18.28	2.737
85.06	83.16	260.58	205.5	20.31	3.978
91.16	90.55	265.72	207.4	22.60	5.616
97.23	97.46	271.04	210.9	25.16	7.759
103.23	104.0	276.36	210.9	28.03	10.47
109.18	110.3	281.69	212.3	31.24	13.83
114.81	116.1	286.96	213.9	34.84	17.94
120.14	121.3	292.20	215.5	38.84	22.97
125.44	126.5	297.42	217.3	43.32	28.36
130.69	131.3	302.62	218.5	48.34	34.42
135.92	135.9	307.79	219.5	53.90	41.87
				59.98	49.94
				66.29	58.43

fits the data with an average deviation 0.8%. Both equations yield values for the specific heat of cryolite in J/(g K).

The enthalpy of the α-β transition may be calculated from the difference between the measured heat capacities and the two equations given above. Our estimate of the enthalpy of the α-β transition in cryolite is 8.78 $\pm$ 1.2 kJ. This value compares favorably with published values of O'BRIEN and KELLEY (1957; 9.04 kJ) and STULL and PROPHET (1971; 8.24 $\pm$ 1.67 kJ), but is somewhat smaller than the value of 9.5 $\pm$ 1.7 kJ reported by CHASE *et al.* (1985). Each value is dependent upon the equations used in the respective studies to smooth the experimental data.

Correlation of transitional enthalpy and temperature values

The α-β transition of pure cryolite represents a fixed physical point, regardless of the apparent temperatures reported. There has, however, been a great deal of discussion in the literature on the temperature and enthalpy of this transition. O'BRIEN and KELLEY (1957) report a value of 845 K for the α-β transition in cryolite, and their calculated enthalpy value for β-cryolite at the transition temperature differs from that calculated here by 0.16%, less than the uncertainty in either data set.

The enthalpy value reported by ALBRIGHT (1956) is about 0.2% larger than our value. However, he did not independently define the temperatures for the α-β and melting transitions, but chose them to be consistent with the values given by STEWARD and ROOKSBY (1953) and used in the Aluminum Research Laboratory (ROLIN, 1952), and did not explain how his data were adjusted to these values. The temperature assigned to the α-β transition by Steward and Rooksby was based upon X-ray data from a 19 cm diameter UNICAM high temperature powder camera. The uncertainty in the temperature is not known.

FRANK (1961) noted the difference between the α-β transition and fusion temperatures for cryolite reported by O'BRIEN and KELLEY (1957) and ALBRIGHT (1956). Frank concluded that the temperature scale used by O'Brien and Kelley was in error by 21 K at 1300 K, and suggested that a correction be made to the data of O'Brien and Kelley based upon a linearly increasing temperature error of 0 K at 298.15 K and

Table 3. Comparison of heat capacity determinations on cryolite

T	Cp (J/mol K) (1)	(2)	(3)	Percent deviation	
(K)	U.S.G.S. (This Study)	U. Michigan (This Study)	U.S.B.M. (King, 1957)	(1)-(2)	(1)-(3)
50	36.7	37.2	37.6	-1.40	-2.50
100	100.4	100.4	99.8	0.00	-0.57
150	147.4	147.5	147.3	-0.07	-0.08
200	179.5	179.8	179.0	-0.16	0.28
250	201.9	201.9	200.8	0.00	0.53
298.15	217.1	217.7	215.9	-0.28	0.55

Table 4. Experimental superambient heat capacities of cryolite determined by DSC

T	C_p	T	C_p	T	C_p
K	J/(mol K)	K	J/(mol K)	K	J/(mol K)
Series I		Series V		Series X	
340.2	225.1	659.4	273.1	848.0	283.0
360.2	229.3	679.4	275.0		
380.1	233.9	699.3	279.6	Series XI	
400.1	238.1	719.3	283.4		
420.0	241.0	739.3	289.1	848.0	283.6
440.0	243.3	748.2	292.7		
459.9	245.8			Series XII	
479.9	248.6	Series VI			
499.8	251.1			833.0	503.4
519.8	253.8	769.2	298.3	833.5	604.8
539.7	256.5	779.2	305.7	834.0	802.6
548.7	257.6	789.1	311.1	834.5	1448.2
		798.1	315.1	835.0	2765.1
Series II				835.5	3936.2
		Series VII		836.0	4375.0
420.0	239.8			836.5	4426.8
440.0	242.9	809.1	317.2	837.0	591.4
459.9	245.4	811.1	318.5	837.5	307.8
479.9	248.4	813.1	320.6	838.0	297.9
499.8	251.9	815.1	323.1	838.5	300.0
519.8	254.0	817.1	326.7	839.0	288.5
539.7	257.6	819.1	329.0	839.5	292.2
548.7	259.3	821.1	333.6	840.0	285.3
		823.1	338.2		
Series III		825.0	343.9	Series XIII	
		827.0	349.8		
519.8	253.6	829.0	357.1	868.9	280.3
539.7	256.1	831.0	367.0	878.9	280.7
559.7	257.8	843.0	284.3	888.9	280.5
579.6	260.5	845.0	283.2	897.9	280.3
599.6	263.3	847.0	281.5		
619.5	267.0	848.0	280.9	Series XIV	
639.5	270.0				
648.5	273.6	Series VIII		997.5	281.5
		947.8	280.1		
Series IV					
		Series IX			
459.9	246.9				
479.9	247.7				
549.7	256.8	947.8	280.7		
558.7	259.1				

Table 5. Smoothed superambient thermodynamic functions for cryolite at selected temperatures

T	C_p	$S^0_T - S^0_0$	$(H^0_T - H^0_{298})/T$	$-(G^0_T - H^0_{298})/T$	ΔG^0_T(f,elem)
K	J/(mol K)	J/(mol K)	J/(mol K)	J/(mol K)	kJ/mol
298.15	217.4	238.5	0.000	238.5	-3144.92
300	217.8	239.8	1.342	238.5	-3143.92
350	228.8	274.2	33.037	241.2	-3116.42
400	238.8	305.5	58.161	247.3	-3088.43
450	246.1	334.0	78.661	255.4	-3060.08
500	251.6	360.3	95.692	264.6	-3031.84
550	256.5	384.5	110.09	274.4	-3003.74
600	262.3	407.0	122.52	284.5	-2975.80
650	270.1	428.3	133.56	294.8	-2948.05
700	281.1	448.7	143.68	305.0	-2920.49
750	296.1	468.6	153.32	315.3	-2893.14
800	316.0	488.3	162.84	325.5	-2866.02
836.5	333.9	502.9	169.90	332.9	-2846.36
836.5	276.8	512.7	179.80	332.9	-2846.36
850	277.5	517.1	181.35	335.8	-2839.27
900	279.9	533.1	186.75	346.3	-2813.09
950	282.3	548.3	191.72	356.5	-2796.86
1000	284.7	562.8	196.31	366.5	-2760.38
1050	287.1	576.7	200.57	376.2	-2734.04
1100	289.5	590.2	204.56	385.6	-2707.84
1150	291.9	603.1	208.30	394.8	-2681.78
1153	292.0	603.8	208.52	395.3	-2680.22
1153	300.4	605.6	210.34	395.3	-2680.22
1200	300.4	617.6	213.87	403.7	-2649.70
1250	300.4	629.9	217.33	412.5	-2611.60
1290	300.4	639.3	219.91	419.4	-2578.98
1290	394.7	727.3	308.09	419.4	-2578.98
1300	394.7	730.5	308.76	421.8	-2574.56
1350	394.7	745.4	311.94	433.5	-2541.35
1400	394.7	759.8	314.89	444.9	-2508.49

21 K at 1300 K. He corrected values for cryolite, AlF_3 and NaF on this basis. DOUGLAS and DITMARS (1967) questioned the corrections proposed by FRANK (1961), and stated that their results for the enthalpy of AlF_3 compared more favorably with the original values reported by O'BRIEN and KELLEY (1957) than with the corrected values given by FRANK (1961). STULL and PROPHET (1971) and ROBIE *et al.* (1979) followed the suggestions of Douglas and Ditmars and did not correct the enthalpy data of O'Brien and Kelley for either AlF_3 or cryolite.

Our results for cryolite, combined with our analysis of the transition temperatures for cryolite, suggest that the temperature scale used by O'BRIEN and KELLEY (1957) was in error. DOUGLAS and DITMARS (1967) based their conclusion regarding the temperature scale used by O'Brien and Kelley upon the temperatures cited for the α-β transition in AlF_3 and on a comparison of the heat capacities calculated from each of the enthalpy data sets.

The α-β transition in AlF_3 has a measured enthalpy of transition of about 560 J/mol (DOUGLAS and DITMARS, 1967). O'BRIEN and KELLEY (1957) placed the transition at 727 K based upon enthalpy measurements at 724.9 and 728.1 K. Douglas and Ditmars found the α-β transition in their sample occurred gradually between 723 and 726 K. Correcting for impurities yielded a transition temperature of 728 K for pure AlF_3. The sample studied by O'Brien and Kelley had a similar chemical composition and yielded a similar temperature for the α-β transition in AlF_3. This conformity may be somewhat fortuitous as DOUGLAS and DITMARS (1967) showed that once the sample has been converted to β-AlF_3, it may be cooled at least 6 K without undergoing a transition back to α-AlF_3. Therefore, the value obtained by O'Brien and Kelley at 728.1 K for the β-AlF_3 phase may not represent the temperature limit assumed in calculating the transition temperature, because O'Brien and Kelley were unaware of the hysteresis in that transition. The data of O'Brien and Kelley limit the transition to between 724.9 and 734 K on their temperature scale.

The values for the temperature of the transition reported by O'BRIEN and KELLEY (1957) and DOUGLAS and DITMARS (1967) are substantially different from the value calculated by FRANK (1961). The measured enthalpy data as a function of temperature are also different. Using the data of DOUGLAS and DITMARS (1967) as the reference data set, the results of O'Brien and Kelley are less than the reference set by −0.15% at 400 K, and −0.8% at 1400 K. The data given by FRANK (1961) are about 0.8% higher than the reference set at 400 K and rise gradually to 1.6% greater at 1400 K. Clearly, the slope of the data set of Douglas and Ditmars is different than that of the other two data sets.

Given these results, we suggest that the temperature scale used by O'BRIEN and KELLEY (1957) is in error, but by a lesser amount than that estimated by FRANK (1961). The α-β transition in cryolite is a better reference point for the temperature scales than is the α-β transition in AlF_3 because of the hysteresis problem in AlF_3. The value observed in our data set yields an estimated error with respect to our temperature scale of +5.5 K in the O'BRIEN and KELLEY (1957) temperature scale at 850 K and an error of +10 K at 1300 K assuming the correction increases linearly with the temperature from 0 at 298.15 K. This interpretation moves the transition temperature of O'Brien and Kelley from 845 K to 842 K based upon the observed pretransition effect reported by O'Brien and Kelley at 839.9 K and the observed half-width of the heat capacity anomaly observed here (2 K). The corrected enthalpy at 1300 K differs from the values obtained by HOLM and GRØNVOLD (1973) by 0.16%. In all cases the uncorrected data of O'Brien and Kelley are significantly different from the results presented in other studies. As the corrections provide a better agreement this suggests that the correction is reasonable.

The size of the temperature correction is consistent with the findings of MCADIE *et al.* (1972) who reported transition temperatures for ten materials for the Standards Committee of the International Confederation on Thermal Analysis. MCADIE *et al.* found that the standard deviations, based upon the mean values from the 34 participating laboratories, were 5 to 8 K for transitions at temperatures between 400 and 1250 K. As the data of MCADIE *et al.* (1972) clearly indicate that temperature scales (calibrated or uncalibrated) can deviate significantly, any evaluation of experimental data from several sources must provide for an analysis of relative differences in the temperature scales. The thermodynamic properties of cryolite (Table 7) are

Table 6. Comparison of reported and adjusted temperatures (in Kelvins) for several transitions in cryolite.

Data Source	Transition Type and Substance: Cryolite α-β	Cryolite Fusion	NaF Fusion	AlF_3 α-β (1)
O'Brien and Kelley (2) (1957)	845	1300	1285	727
Adjusted (3)	836.5	1290	1272	723
Landon and Ubbelohde (1957)	838	1287	1270	-
Albright (1956)	823	1279	--	-
Brynestad et al. (1960)	833	1281	1267	-
Phillips et al. (1955a,b)	-	1282	1267	-
Rolin (1960)	-	1282	1270	-
Clark (1959)	-	--	1265	-
Majumdar and Roy (1965)	835	--	--	-
Roth and Bertram (1929)	838	--	--	-
Douglas and Ditmars (1967)	-	--	--	723
This study	836.5	--	--	-

(1) Transition temperature without correction for impurities (see Douglas and Ditmars, 1967)
(2) Uncorrected Published results
(3) Results corrected by us for temperature error discussed in the text

based upon a temperature scale defined primarily by the melting point for indium and the α-β transition in quartz, both as defined by the International Confederation for Thermal Analysis and by the U.S. National Bureau of Standards (see MCADIE *et al.*, 1972) and released as standard reference materials 758 and 760. Any change in the accepted temperatures for these transitions will alter the thermodynamic properties for cryolite.

We have made several comparisons of the corrected data in support of the arguments for correcting the temperature scale of O'BRIEN and KELLEY (1957). Comparisons of the temperatures for several transitions, reported in the work of O'Brien and Kelley, with data from the literature are given in Table 6. We are aware that impurities within a sample may alter the temperature of a transition. However, the evidence presented in this study strongly suggests that differences resulting from sample impurities are not the major source of the discordances among the enthalpy data of O'BRIEN and KELLEY (1957), ALBRIGHT (1956) and DOUGLAS and DITMARS (1967).

The calorimeter used by O'BRIEN and KELLEY (1957) was described by KELLEY *et al.* (1946). There have been relatively few high-quality measurements in recent years that may be compared with results from their calorimetric system. KELLEY *et al.* reported enthalpy data for silica glass that compare favorably with the recent data of RICHET *et al.* (1982) at 1300 K, but have a different slope in the temperature range 1000 to 1500 K. Nonetheless, it appears that if the results of O'Brien and Kelley for cryolite and AlF_3 are in error it may be limited to a systematic problem in that data set alone.

Smoothed values of the superambient thermodynamic properties of cryolite

The thermodynamic properties of cryolite are listed in Table 5. The entropy at 298.15 K (238.5 J/(mol K)) is calculated from the average of the Michigan and U.S.G.S. low-temperature results. The heat capacity data reported in this study provide the basis for the thermodynamic properties listed between 298.15 and 1000 K. The thermodynamic properties listed at temperatures above 1153 K are based upon the temperature corrected values (discussed above) reported by O'BRIEN and KELLEY (1957). Fitted equations are given in Table 8 and in an earlier section of this paper. For these purposes, the two sets of data provided by LANDON and UBBELOHDE (1957) will be accepted as defining a premelting transition at about 1153 K. The temperature of fusion of cryolite is taken as 1290 K from the corrected results of O'BRIEN and KELLEY (1957).

The enthalpy and entropy of the α-β transition in cryolite calculated from the data in Table 8 are 8.775 kJ/mol and 10.5 J/(mol K), respectively, at 836.5 K. The β-γ cryolite transition at 1153 K has an enthalpy and entropy of transition of 2.098 kJ/mol and 1.8 J/(mol K). The enthalpy and entropy of fusion at 1290 K are 113.75 kJ/mol and 88.2 J/(mol K). These results are significantly different from those given by STULL and PROPHET (1971), ROBIE *et al.* (1979) and CHASE *et al.* (1985) who derived enthalpies about one percent lower at the higher temperatures. The major source for this discrepancy is the treatment given to the data of O'BRIEN and KELLEY (1957).

PHASE EQUILIBRIA IN THE SYSTEM Na-Fe-Al-Si-O-F

The heat capacity data for cryolite presented above may be used to constrain phase relations for the system Na-Fe-Al-Si-O-F. This system is useful for constraining the conditions of formation of several natural rock

Table 7. Comparison of smoothed thermophysical properties of cryolite at low-temperatures.

T (K)	$S_T - S_0$ J/(mol K)				$(H_T - H_0)/T$ J/(mol K)		
	U.S.G.S.	U. Mich	Adopted	U.S.B.M.	U.S.G.S.	U. Mich	Adopted
	This Study			King (1957)	This Study		
50	15.87	16.01	15.94	--	11.56	11.67	11.62
100	61.42	61.88	61.65	--	40.49	40.76	40.63
150	111.6	112.1	111.8	--	68.77	68.95	68.86
200	158.7	159.2	159.0	--	92.70	92.89	92.80
250	201.3	201.8	201.6	--	112.4	112.6	112.5
298.15	238.2	238.9	238.5	238 ± 2	128.2	128.3	128.2
350	274.0	274.8	274.4	--	142.3	142.6	142.4

types, and forms a basis from which a more complete diagram involving Ca, K and H may be derived. Twenty-seven selected phases are considered: cryolite (Cy), chiolite (Ci), villiaumite (Vl), quartz (Qz), albite (Ab), nepheline (Ne), natrosilite (Ns), corundum (Co), Na_2SiO_3 (sodium metasilicate, Nm), sillimanite (Sl), andalusite (And), fluortopaz (Tp), AlF_3, SiF_4(g), SiF_3(g), SiF_2(g), SiF(g), hematite (Hm), magnetite (Mt), fayalite (Fa), wüstite (Wu), iron (Fe), almandine (Alm), hercynite (Hc), FeF_2, FeF_3, and acmite (Ac, aegirine: see Table 9). Many other phases have been excluded, including malladrite (Na_2SiF_6) and iron-cordierite ($Fe_2Al_4Si_5O_{18}$), for which no adequate thermodynamic data exist, jadeite, which is only stable at high pressures, and various synthetic compounds unknown as minerals. In the absence of cordierite, its place is taken by the assemblage hercynite-quartz. In addition, possible solid-solutions, such as $\square Si_2O_4$ in nepheline, $FeAl_2O_4$ in magnetite and $NaAlSi_2O_6$ in aegirine, have been ignored. All calculations have been performed at temperatures where andalusite is the stable aluminosilicate polymorph. Calculations using sillimanite, however, show that the choice of polymorph makes little difference in the temperature range investigated here (600–1050 K). As the pressure effects on most of the reactions discussed here are small, these diagrams should be qualitatively correct at somewhat higher pressures.

Data for the calculations presented here were derived from standard compilations with the exception of cryolite, high albite, fluortopaz, hercynite, and acmite (Table 9). The heat capacity and Gibbs' energy of cryolite were calculated from our measured entropy and the enthalpy data tabulated by ROBIE *et al.* (1979). The molar volume for the high temperature polymorph of cryolite was derived from unpublished data on the molar volume of cryolite as a function of temperature provided by D. R. Peacor of the University of Michigan. The Gibbs' energy of albite was calculated from the entropy data of HASELTON *et al.* (1983) and the enthalpy data of ROBIE *et al.* (1979). High temperature entropy data for hercynite were obtained from our own unpublished DSC results. The entropy of hercynite at STP and its Gibbs energy were fitted to the experimental reversals of BOHLEN *et al.* (1986) on the reaction

$$3\ \text{Hercynite} + 5\ \text{Quartz} = \text{Almandine} + 2\ \text{Sillimanite} \quad (3)$$

using the data for almandine, quartz and sillimanite given by ANOVITZ and ESSENE (1987). The heat capacity data for acmite (KO *et al.*, 1977) were combined with solution calorimetry data (BENNINGTON, 1981) to yield $\Delta G^0_{298} = -2410.42$ kJ/mole for acmite. The heat capacity of chiolite is taken from STUVE and FERRANTE (1980), and its Gibbs energy is taken from JANAF (CHASE *et al.*, 1985) which is based on the solid electrolyte measurements of DEWING (1970).

The system Na-Al-Si-O-F

Stable equilibria in the system Na-Fe-Al-Si-O-F are calculated at 1000 K and 1 bar (Fig. 1). Because of the complexity of this and other phase diagrams presented below it was not possible to label all reactions directly on the figures, but they are listed in Table 10. Not shown in Fig. 1 is the reaction

$$4\ \text{Na-metasilicate} + 2\ \text{Corundum} + 2\ F_2 = 4\ \text{Nepheline} + 4\ \text{Villiaumite} + O_2 \quad (4)$$

which lies at fF_2 values too low to be shown.

Phases in the system Na-Al-Si-O-F may be represented in composition space as a right triangular prism (Fig. 2) following KOGARKO (1966). Only that portion of this space containing solid phases considered here is shown. Tie lines connect phases which coexist at 1 bar and 1000 K, and outline stable solid phase assemblages allowed by Fig. 1. By projecting this diagram through O_2 (or F_2) Na-Al-Si triangles are obtained that represent the sequence of reactions with changing fO_2/fF_2 (Fig. 3).

Several phase incompatibilities are evident in Fig. 3. Chiolite is stable only at very high fluorine fugacities and is not stable with natrosilite ($Na_2Si_2O_5$), Na-metasilicate (Na_2SiO_3), nepheline, andalusite, villiaumite, or albite. On the basis of a schematic derivation of phase equilibria in this system, BURT (1979) states that fluortopaz is incompatible with nepheline or villiaumite, which is supported by our calculations. Natrosilite ($Na_2Si_2O_5$) is known from only one locality, Lovozero on the Kola peninsula of the USSR (TIMOSHENKOV *et al.*, 1975), and Na_2SiO_3 is unknown as a mineral. The stabilities of these phases are presumably limited in nature both by their high solubilities and their decomposition at very low fluorine fugacities.

Cryolite is stable over a wide range of fO_2/fF_2 conditions, but it has a more limited stability in the presence of quartz, fluortopaz, corundum, or albite. Cryolite is absent from most undersaturated alkalic rocks. Kogarko suggests that the assemblage albite-nepheline-

Table 8. Heat-capacity equations for crystalline and liquid cryolite

Phase	Temperature Range (K)	C_p J/(mol K)
α - cryolite	270 - 836.5	$3617.59 - 3.40859(T) + 1.77182 \times 10^{-3}(T)^2 - 4.97563 \times 10^{4}(T)^{-0.5} + 3.0087 \times 10^{7}(T)^{-2}$
β - cryolite	836.5 - 1153	$236.69 + 4.7986 \times 10^{-2}(T)$
γ - cryolite	1153 - 1290	300.41
liquid cryolite	1290 - 1400	394.68

Table 9. Thermodynamic data for selected phases in the system Na-Fe-Al-Si-O-H.

Phase	Formula	Abb.	Volume	S^0(298 K)	A	B	C	D	ΔG^0(298 K)	Sources
			cm^3	J/(mol K)					kJ/mol	
α-Cryolite	Na_3AlF_6	α-Cy	70.81	238.45	145.1140	193.0095	-10.3661	-872.89	-3152.17	1,2,3,4,11
β-Cryolite	Na_3AlF_6	β-Cy	72.31	238.45	198.4141	73.2027	-63.8138	-1113.11	-3145.54	1,2,3
Chiolite	$Na_5Al_3F_{14}$	Ci	154.03	483.54	510.7367	87.2356	36.8953	-2977.52	-7200.35	1,5,6,7,8,11
Villiaumite	NaF	Vl	14.98	51.21	38.7239	21.0355	-1.7476	-224.98	-545.08	2,9,11
High Albite	$NaAlSi_3O_8$	Ab	100.43	225.70	278.6331	41.8797	42.7479	-1647.98	-3706.30	2,10
Nepheline	$NaAlSiO_4$	Ne	54.16	124.35	144.7547	32.5419	14.0394	-850.31	-1977.48	2
Natrosilite	$Na_2Si_2O_5$	Ns	71.69	164.05	159.2248	104.4691	13.2125	-953.52	-2324.16	12,11
Na-metasilicate	Na_2SiO_3	NM	46.49	113.85	120.7804	50.9771	9.7194	-714.58	-1467.33	13,11
Fluortopaz	$Al_2SiO_4F_2$	Tp	51.61	105.40	177.6215	55.4555	21.0522	-1052.50	-2910.66	14
AlF_3	AlF_3	AlF_3	26.15	66.48	47.0943	84.5549	-3.0221	-290.15	-1431.07	2,9
AlF_3	AlF_3	AlF_3	26.21	66.48	129.7659	-12.6624	79.3601	-778.74	-1426.28	2,9,15,16
SiF_4(g)	SiF_4	SiF_4		282.76	95.5887	6.8937	9.8496	-558.64	-1572.71	11
SiF_3(g)	SiF_3	SiF_3		282.38	77.5126	3.4096	9.6373	-453.45	-1073.22	11
SiF_2(g)	SiF_2	SiF_2		256.58	55.0714	1.9016	5.6695	-320.70	-598.28	11
SiF(g)	SiF	SiF		225.79	35.9427	1.2383	1.9461	-207.34	-51.56	11
Quartz	SiO_2	Qz	22.69	41.46	73.4890	0.7849	15.3766	-436.14	-856.29	2
Corundum	Al_2O_3	Co	25.57	50.92	116.3382	11.9809	19.5146	-588.29	-1572.58	2
Andalusite	Al_2SiO_5	And	51.56	91.49	175.3450	21.9060	27.7269	-1036.69	-2444.56	17,18
Sillimanite	Al_2SiO_5	Sl	50.02	95.80	169.4389	28.9046	25.6209	-1002.81	-2440.74	17,18
Iron	Fe	Fe	7.09	27.28	-0.7391	48.1793	-6.3572	3.04	0	19
Magnetite	Fe_3O_4	Mt	44.52	146.15	318.6083	-80.1150	84.6452	-1885.38	-1012.90	19
Hematite	Fe_2O_3	Hm	30.27	87.48	95.7822	-79.1900	5.4342	-572.02	-745.27	19
Wustite	$Fe_{0.947}O$	Wu	12.04	57.57	44.9390	11.2072	-1.5885	-257.69	-245.15	19
Fayalite	Fe_2SiO_4	Fa	46.39	152.13	156.6201	35.0661	15.6201	-920.44	-1380.22	19
FeF_2(c)	FeF_2	FeF_2	22.02	86.99	75.4189	7.5574	4.9125	-437.47	-663.17	11,22
FeF_3(c)	FeF_3	FeF_3	31.50	98.32	77.8722	4.3345	6.4819	-452.26	-972.29	11,23
Hercynite	$FeAl_2O_4$	Hc	40.75	121.34	125.9425	65.3457	7.8140	-746.09	-1838.58	1
Acmite	$NaFeSi_2O_6$	Ac	64.60	148.20	214.7666	45.1046	28.3368	-1268.82	-2410.42	20,21,24

Thermodynamic properties used in these calculations. 1) This study, 2) Robie et al. (1979), 3) Peacor (unpb.), 4) S^0_{298} arbitrarily chosen to fit entropy above transition, 5) Stuve and Ferrante (1980), 6) Clausen (1936), 7) Brosset (1938), 8) Dewing (1970), 9) CODATA (1977), 10) Haselton et al. (1983), 11) Chase et al. (1985), 12) Timoshenkov et al. (1975), 13) Grund and Pizy (1952), 14) Barton (1982), Barton et al., (1982), 15) Douglass and Ditmars (1967), 16) Skinner (1966), 17) Anovitz et al. (1987), 18) Robie and Hemingway (1984), 19) Robinson et al. (1982), 20) Ko et al. (1977), 21) Bennington (1981), 22) JCPDS, Card No. 18-638, 23) Ebert (1931), 24) Hemingway (unpb.)

$$S^0_T - S^0_{298} = A\ln T + B\,10^{-3}T + C\,10^5/T^2 + D$$

villiaumite must be stable instead of the cryolite-bearing assemblages (Cy-Ab-Ne and Cy-Ab-Vl) on the basis of the occurrence of the assemblage nepheline-albite-villiaumite in nepheline syenites (Lovozero, USSR: VLASOV *et al.*, 1966; Ilimaussaq, Greenland: BONDAM and FERGUSON, 1962; Iles de Los, French Guinea:

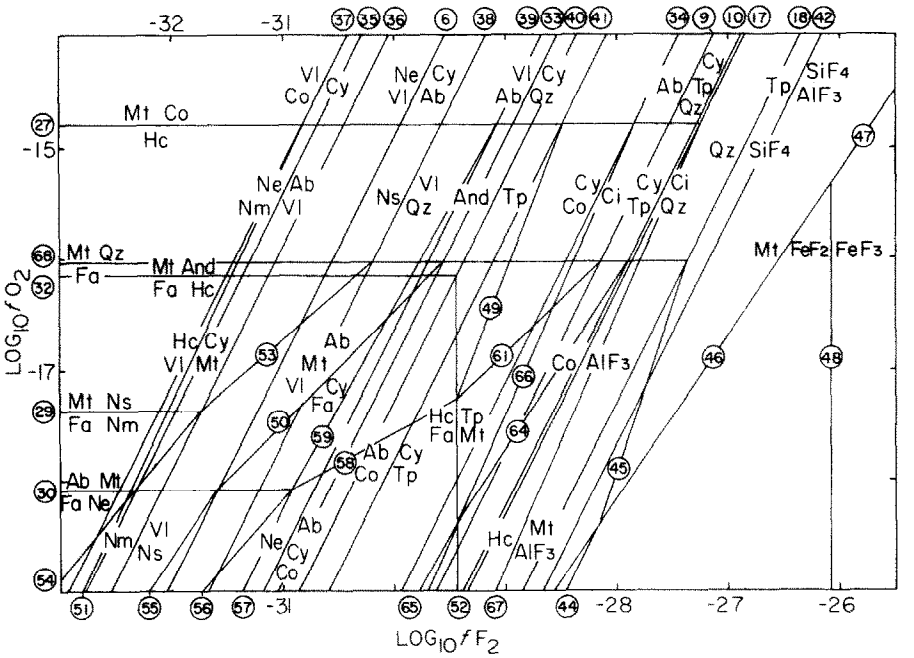

FIG. 1. Phase equilibria in the system Na-Fe-Al-Si-O-F in fO_2-fF_2 space at 1000 K and 1 bar. Reactions involving SiF_4 and AlF_3 are calculated assuming the fugacities of these fluids to be 1.

Table 10. Reactions in the system Na-Fe-Al-Si-O-F. Reaction numbers as referred to in text and figures 1, 5 and 7.

3) 3 Hc + 5 Qz = Alm + 2 Sil

4) 4 Nm + 2 Co + 2 F_2 = 4 Ne + 4 Vl + O_2

6) 3 Ne + 4 Vl + 4 F_2 = 2 Cy + Ab + 2 O_2

7) 2 Ab + 2 F_2 = 2 Vl + Tp + 5 Qz + O_2

8) 5 Ab + 8 F_2 = Ci + Tp + 14 Qz + 4 O_2

9) 3 Ab + 4 F_2 = Cy + Tp + 8 Qz + 2 O_2

10) 5 Cy + 2 Tp + 4 F_2 = 3 Ci + 2 Qz + 2 O_2

11) 7 Cy + 3 Tp + 4 F_2 = 4 Ci + Ab + 2 O_2

12) Cy + 2 Ab + 4 F_2 = Ci + 6 Qz + 2 O_2

15) 5 Ab + 8 F_2O_{-1} = Ci + Tp + 14 Qz

17) 2 Co + 6 F_2 = 4 AlF_3 + 3 O_2

18) Qz + 2 F_2 = SiF_4(g) + O_2

19) 2 Qz + 3 F_2 = 2 SiF_3(g) + 2 O_2

20) Qz + F_2 = SiF_2(g) + O_2

21) 2 Qz + F_2 = 2 SiF + 2 O_2

22) 12 Ac + 3 Cy = 18 Vl + 4 Mt + 3 Ab + 15 Qz + O_2

23) 6 Ac + 3 Ab + 9 F_2 = 3 Cy + 21 Qz + 2 Mt + 5 O_2

24) 12 Ac = 6 Ns + 4 Mt + 12 Qz + O_2

25) 4 Ac + 3 Ne = 3 Ab + 2 Hm + 2 Nm

26) Mt + 3 Fe + 2 O_2

27) 2 Mt + 6 Co = 6 Hc + O_2

28) 2 Mt + 6 And = 6 Hc + 6 Qz + O_2

29) 2 Mt + 3 Ns = 3 Fa + Nm + O_2

30) 4 Mt + 3 Ab = 6 Fa + 3 Ne + 2 O_2

31) 2 Hc + 3 Qz = Fa + 2 And

32) 2 Mt + 2 And = 2 Fa + 2 Hc + O_2

33) Cy + 3 Qz + O_2 = 2 Vl + Ab + 2 F_2

34) 3 Ci + 3 O_2 = 5 Cy + 2 Co + 6 F_2

35) Ne + 2 Nm + 2 F_2 = Ab + 4 Vl + O_2

36) 4 Nm + 2 F_2 = 4 Vl + 2 Ns + O_2

37) 12 Vl + 2 Co + 6 F_2 = 4 Cy + 3 O_2

38) 2 Ns + 2 F_2 = 4 Vl + 4 Qz + O_2

39) 9 Ne + 6 F_2 = 3 Ab + 2 Cy + 2 Co + 3 O_2

40) 2 And + 2 F_2 = 2 Tp + O_2

41) 3 Ab + 8 Co + 12 F_2 = Cy + 9 Tp + 6 O_2

42) Tp + 4 F_2 = SiF_4 + 2 AlF_3 + 2 O_2

43) Tp + 2 F_2 = Qz + 2 AlF_3 + O_2

44) Fa + 4 F_2 = 2 FeF_2 + SiF_4 + 2 O_2

45) 3 Fa + 6 F_2 = 2 Mt + 3 SiF_4 + 2 O_2

46) Mt + 3 F_2 = 3 FeF_2 + 2 O_2

47) 2 Mt + 9 F_2 = 6 FeF_3 + 4 O_2

48) 2 FeF_2 + F_2 = 2 FeF_3

49) 24 Hc + 9 Ab + 27 F_2 = 3 Cy + 27 Tp + 8 Mt + 14 O_2

50) Ab + 2 Mt + 2 Vl + 2 F_2 = Cy + 3 Fa + 2 O_2

51) 3 Hc + 18 Vl + 9 F_2 = 6 Cy + Mt + 4 O_2

52) Hc + Fa + F_2 = Tp + Mt + O_2

53) 8 Mt + 6 Ns + 6 F_2 = 12 Fa + 12 Vl + 7 O_2

54) 4 Mt + 6 Nm + 6 F_2 = 6 Fa + 12 Vl + O_2

55) 2 Mt + 6 Vl + 3 Ne + 6 F_2 = 3 Cy + 3 Fa + 4 O_2

56) 9 Ne + 7 Mt + 9 F_2 = 3 Hc + 9 Fa + 3 Cy + 8 O_2

57) 19 Ne + 2 Fa + 12 F_2 = 4 Hc + 7 Ab + 4 Cy + 6 O_2

58) 9 Ab + 19 Mt + 9 F_2 = 3 Hc + 3 Cy + 27 Fa + 14 O_2

59) 27 Ne + 2 Mt + 18 F_2 = 6 Hc + 9 Ab + 6 Cy + 10 O_2

60) 16 Hc + 9 Ab + 28 F_2 = 19 Tp + 3 Cy + 8 Fa + 14 O_2

61) 9 Ab + 16 Mt + 12 F_2 = 3 Tp + 3 Cy + 24 Fa + 14 O_2

62) 2 Ab + 4 Mt + Cy + 2 F_2 = 6 Fa + Ci + 4 O_2

63) 15 Ab + 29 Mt + 18 F_2 = 3 Tp + 42 Fa + 3 Ci + 26 O_2

64) 4 Mt + 6 Tp + 15 Cy + 12 F_2 = 9 Ci + 6 Fa + 8 O_2

65) 2 Hc + 15 Cy + 2 Tp + 16 F_2 = 9 Ci + 2 Fa + 8 O_2

66) 6 Hc + 15 Cy + 18 F_2 = 9 Ci + 2 Mt + 8 O_2

67) 3 Hc + 9 F_2 = 6 AlF_3 + Mt + 4 O_2

68) 3 Fa + O_2 = 2 Mt + 3 Qz

69) 4 Mt + O_2 = 6 Hm

70) 2 Ac + 2 Nm = Hm + 3 Ns

71) 2 Ac + 2 Co = Hm + Ns + 2 And

72) 12 Ac + 12 Nm = 4 Mt + 18 Ns + O_2

73) 12 Ac + 12 Co = 4 Mt + 6 Ns + 12 And + O_2

74) 12 Ac + 12 Hc + O_2 = 8 Mt + 12 And + 6 Ns

75) 4 Ac = 2 Fa + 2 Qz + 2 Ns + O_2

76) 12 Ac + 4 Hc = 4 And + 8 Fa + 6 Ns + 3 O_2

77) 4 Ac + 2 Nm = 4 Ns + 2 Fa + O_2

78) 12 Ac + 8 Mt = 12 Fa + 6 Nm + 7 O_2

79) 12 Ac + 4 Mt = 6 Ns + 12 Fa + 5 O_2

80) 12 Ac + 9 Ne = 9 Ab + 4 Mt + 6 Nm + O_2

81) 2 Hm + 6 F_2 = 4 FeF_3 + 3 O_2

82) 2 Hm + 4 Ns + 2 F_2 = 4 Ac + 4 Vl + O_2

83) 4 Ac + 2 F_2 = 2 Hm + 4 Vl + 8 Qz + O_2

84) 12 Ac + 18 Co = 4 Mt + 18 And + 6 Nm + O_2

85) 4 Ac + 10 Co = 4 Hc + 6 And + 2 Nm + O_2

86) 5 Mt + 9 And + 3 Nm = 6 Ac + 9 Hc + O_2

87) 4 Ac + 8 Nm + 4 And = 4 Hc + 10 Ns + O_2

88) 2 Mt + 6 Nm + 6 And = 6 Hc + 6 Ns + O_2

89) And + Nm = Co + Ns

90) 12 Ac + 8 Hc = 6 Nm + 10 Fa + 8 And + 3O_2

91) 3 Ns + 2 Hc = 3 Nm + Fa + 2 And

92) 2 Ac = Hm + Ns + 2 Qz

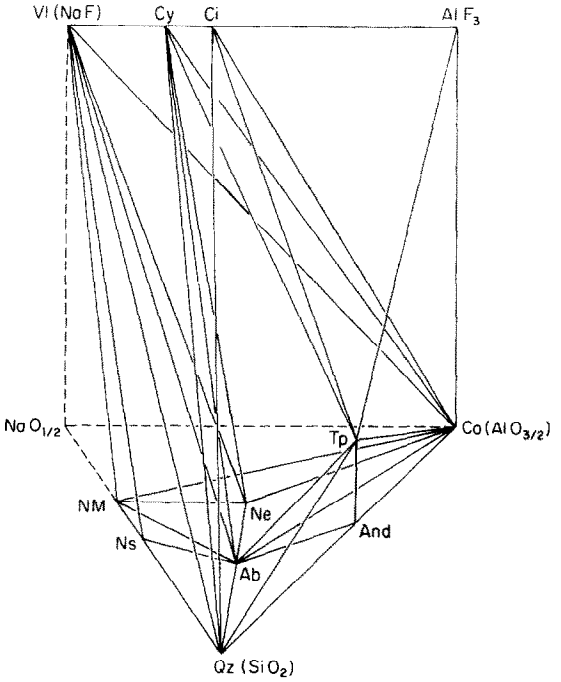

FIG. 2. Coexisting solid phases in the system Na-Al-Si-O-F at 1000 K, 1 bar, shown in the composition space AlF_3-NaF-SiO_2-$AlO_{3/2}$-$NaO_{1/2}$.

LACROIX, 1908). She notes, however, that the Gibbs' energy of reaction (5)

$$2\ \text{Cryolite} + \text{Albite} + 4\ H_2O = 3\ \text{Nepheline} + 4\ \text{Villiaumite} + 8\ HF \quad (5)$$

is positive at 1 bar, 600°C, and that cryolite-albite bearing assemblages are therefore more stable than the nepheline-villiaumite bearing ones more commonly reported. This argument ignores the effects of variable fluid compositions on mineral stabilities in this system. In our water-free system, reaction (5) is represented by

$$2\ \text{Cryolite} + \text{Albite} + 2\ O_2 = 3\ \text{Nepheline} + 4\ \text{Villiaumite} + 4\ F_2. \quad (6)$$

Reaction (6) implies that the nepheline-albite-villiaumite assemblage noted by Kogarko is stabilized by oxygen fugacities too high or fluorine fugacities too low to stabilize cryolite (Figs. 1, 3).

The calculations also suggest that the albite-quartz-sillimanite-cryolite (or villiaumite) assemblage occasionally used as an experimental HF buffer must be metastable (BURT, 1979; Fig. 3; BURT and LONDON, 1982). In addition, not shown on our diagrams are the metastable reactions:

$$2\ \text{Albite} + 2\ F_2 = 2\ \text{Villiaumite} + \text{Fluortopaz} + 5\ \text{Quartz} + O_2 \quad (7)$$

and

$$5\ \text{Albite} + 8\ F_2 = \text{Chiolite} + \text{Fluortopaz} + 14\ \text{Quartz} + 4\ O_2 \quad (8)$$

both of which occur at fF_2 values above the stable reaction

$$3\ \text{Albite} + 4\ F_2 = \text{Cryolite} + \text{Fluortopaz} + 8\ \text{Quartz} + 2\ O_2. \quad (9)$$

Because reaction (7) is metastable relative to reaction (9) and occurs at conditions where fluortopaz is stable instead of sillimanite (or andalusite), Burt's conclusion that the albite-quartz-sillimanite-villiaumite assemblage is metastable must be correct, as the exchange of sillimanite for fluortopaz in reaction (7) can only generate a reaction which is itself metastable with respect to both reactions (7) and (9).

STORMER and CARMICHAEL (1970) and BURT (1979) have suggested on the basis of natural assemblages that reaction (9) controls the upper stability of albite, and this suggestion is also supported by our calculations. The fF_2 difference between reactions (8) and (9) is, however, only 0.1 log units at 1000 K and 1 bar. Relatively large uncertainties remain in Gibbs' energies of cryolite, chiolite, and villiaumite (±4.2, ±4.6, ±0.7 kJ respectively, ROBIE *et al.*, 1979). These differences are large enough to shift the equilibria in favor of reaction (8). If reaction (8) is indeed stable, reaction (10)

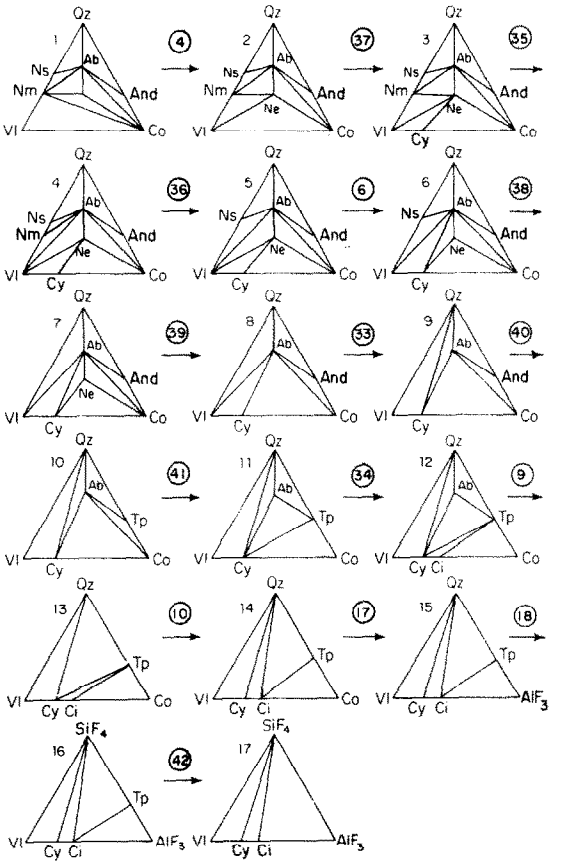

FIG. 3. Projections from excess F_2 and O_2 into Si-Al-Na space, showing the changes in assemblages with increasing fF_2 at 1000 K and 1 bar. The sequence of compatibility triangles represents the successive equilibrium fluoridation of oxides and silicates.

$$5\ \text{Cryolite} + 2\ \text{Fluortopaz} + 4\ F_2 = 3\ \text{Chiolite} + 2\ \text{Quartz} + 2\ O_2 \quad (10)$$

is metastable and

$$7\ \text{Cryolite} + 3\ \text{Fluortopaz} + 4\ F_2 = 4\ \text{Chiolite} + \text{Albite} + 2\ O_2 \quad (11)$$

and

$$\text{Cryolite} + 2\ \text{Albite} + 4\ F_2 = \text{Chiolite} + 6\ \text{Quartz} + 2\ O_2 \quad (12)$$

become stable reactions at fF_2 values below the breakdown of albite.

The relative scarcity of chiolite (BAILEY, 1980) may be explained in terms of the high fluorine fugacities necessary for its stabilization at geologically reasonable fO_2 conditions. At the fF_2 conditions where chiolite becomes stable most fluorine-free silicates have already become unstable. Indeed, SiF_4 fugacities may be high enough (see below) that remaining silicates will begin to vaporize.

Our calculations suggest that the assemblage villiaumite + quartz has a wide stability field (Figs. 1, 3). On the basis of natural assemblages, however, STORMER and CARMICHAEL (1970) suggest that villiaumite and quartz are incompatible. Stormer and Carmichael noted that the stability of villiaumite may be related to the presence of iron-bearing phases. Though their reaction (1) (villiaumite + albite + magnetite = acmite + nepheline) appears to be metastable, the presence of magnetite limits the stability of villiaumite with either nepheline or albite to fO_2 values below the stability limit of cryolite plus quartz at fO_2 values below the QFM buffer. This assemblage strongly restricts, but does not eliminate the stability field of villiaumite plus quartz at 1000 K and 1 bar.

STORMER and CARMICHAEL (1970) suggested that the antipathy between villiaumite and quartz may be due to reaction with plagioclase:

$$2\ \text{Villiaumite} + 4\ \text{Quartz} + \underbrace{\text{Anorthite}}_{(\text{Plagioclase})_{ss}} = 2\ \text{Albite} + \text{Fluorite} \quad (13)$$

Figure 4 (their Fig. 2) shows this reaction using our data, plotting $-\log a(SiO_2)$ as a function of plagioclase composition. The plagioclase activity model of NEWTON *et al.* (1980) were used in this calculation. Reduced silica activity or reduced anorthite content in plagioclase favors the stability of villiaumite (STORMER and CARMICHAEL, 1970). The instability of villiaumite plus quartz in natural Ca-bearing system is thus explained, as only a small anorthite component in the plagioclase is necessary to destabilize the assemblage villiaumite-quartz.

In the system Na-Al-Si-O-F all oxidation and reduction is related to the exchange of oxygen and fluorine. As the oxygen/fluorine charge ratio is fixed at 2:1, all exchange reactions in this system will have two fluorine molecules for every oxygen molecule in the reaction. The slopes of all reactions are therefore parallel in $\log fO_2/\log fF_2$ space and the fugacities of these two fluid components are not independent. BURT (1972) has proposed that both fluorine and oxygen may be represented by the exchange operator F_2O_{-1} which permits consideration of another independent variable on a single two-dimensional diagram. This operator may be defined as

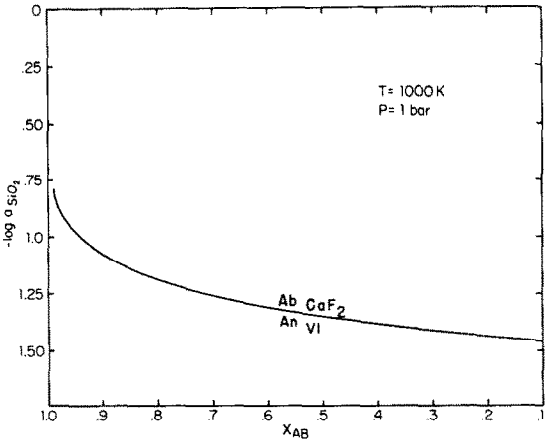

FIG. 4. Reaction (13) at 1000 K and 1 bar plotted as a function of the activity of plagioclase and the activity of quartz. This diagram is a recalculated version of Fig. 2 in STORMER and CARMICHAEL (1970).

$$2\ F_2O_{-1} = 2\ F_2 - O_2. \quad (14)$$

This equation may be added to any reaction of interest. For instance, adding reactions (8) and (14) yields

$$5\ \text{Albite} + 8\ F_2O_{-1} = \text{Chiolite} + \text{Fluortopaz} + 14\ \text{Quartz} \quad (15)$$

for which

$$\log K = -8 \log fF_2O_{-1} = 8 \log (fF_2/(fO_2)^{0.5}). \quad (16)$$

The calculated value of $\log fF_2O_{-1}$ is therefore equal to $\log fF_2$ at $\log fO_2 = 0$.

Figure 5 shows reactions in the system Na-Al-Si-O-F as a function of temperature and fF_2O_{-1}. This diagram has been plotted relative to the reaction

$$2\ \text{Corundum} + 6\ F_2 = 4\ AlF_3 + 3\ O_2 \quad (17)$$

(*cf.* ANOVITZ *et al.*, 1985) in order to allow greater clarity in its presentation. The effects of temperature are quite marked. Plotted reactions have similar fF_2O_{-1}/T slopes except for the quartz – SiF_4(g) and fluortopaz – AlF_3 – SiF_4(g) reactions, which have different slopes due to the participation of additional fluid species.

Silicon-fluoride fugacities

In quartz-bearing rocks, the fugacities of the fluid species SiF_4(g), SiF_3(g), SiF_2(g) and SiF(g) may be readily calculated. Figure 1 shows the limit of stability of quartz at $\log fSiF_4 = 0$ using

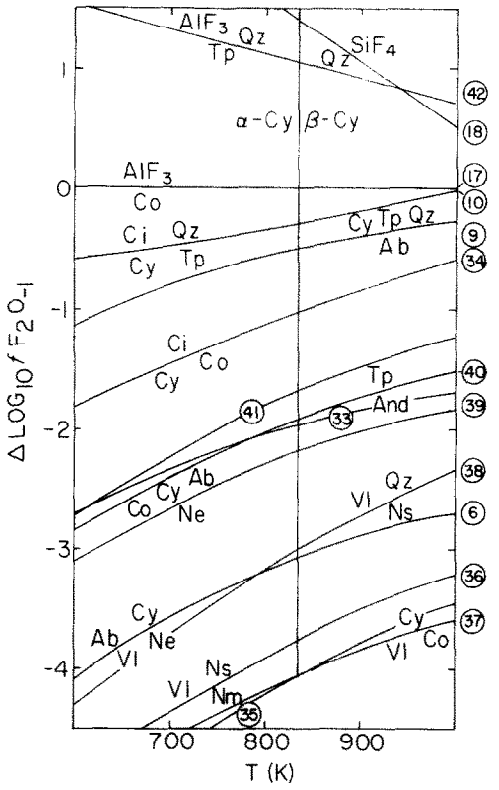

FIG. 5. Effects of temperature on reactions in the system Na-Al-Si-O-F, plotting $\Delta \log fF_2O_{-1}$ ($\Delta \log (fF_2/(fO_2)^{0.5})$) as a function of temperature at 1 bar relative to the reaction of Al_2O_3 to AlF_3 at $fAlF_3 = 1$.

$$\text{Quartz} + 2\ F_2 = SiF_4(g) + O_2, \quad \log_{10} K = 38.7 \quad (1000\ K, 1\ bar). \quad (18)$$

The fugacity of SiF_4 in equilibrium with quartz may be calculated given values for fF_2 and for fO_2. The reactions:

$$2\ \text{Quartz} + 3\ F_2 = 2\ SiF_3 + 2\ O_2; \quad \log_{10} K = 32.6 \quad (1000\ K, 1\ bar) \quad (19)$$

$$1\ \text{Quartz} + F_2 = SiF_2 + O_2; \quad \log_{10} K = -5.8 \quad (1000\ K, 1\ bar) \quad (20)$$

and

$$2\ \text{Quartz} + F_2 = 2\ SiF + 2\ O_2; \quad \log_{10} K = -63.4 \quad (1000\ K, 1\ bar) \quad (21)$$

yield the fugacities of the other silicon-fluoride species in equilibrium with quartz. As expected, these calculations show that SiF_4 is the most important of the silicon fluoride species at fO_2 and fF_2 values of geological interest. Indeed, at the high fF_2/fO_2 implied by the presence of cryolite, significant Si may be transported in the vapor phase as $SiF_4(g)$.

The system Na-Fe-Al-Si-O-F

The addition of iron to Na-Al-Si-O-F allows consideration of additional reactions with iron silicates and iron oxides including hematite, magnetite, fayalite, wüstite, iron, almandine, hercynite and acmite (Fig. 1). Indifferent reactions from the Fe-free system have been omitted. As the calculations (Fig. 6) show that acmite is not stable at 1 bar and 1000 K, no diagram of its stability is presented. The calculations of METZ *et al.* (1983) show that almandine becomes metastable relative to sillimanite, fayalite, and quartz below approximately 2 kbar, and almandine may therefore be ignored in calculations of phase equilibria at 1 bar.

In this system it is no longer possible to use the F_2O_{-1} operator to display gas fugacities as a function of temperature on one diagram, because oxidation and reduction are no longer solely a function of the exchange of oxygen and fluorine. The ratio of F_2 to O_2 is no longer constrained to be 2:1 because iron may be oxidized or reduced in a reaction. The stability of end-member acmite is limited to high fO_2 and low fF_2 (Fig. 6). STORMER and CARMICHAEL (1970) suggested several reactions involving acmite and cryolite, including:

$$12\ \text{Acmite} + 3\ \text{Cryolite} = 18\ \text{Villiaumite} + 4\ \text{Magnetite} + 3\ \text{Albite} + 15\ \text{Quartz} + O_2 \quad (22)$$

and

$$6\ \text{Acmite} + 3\ \text{Albite} + 9\ F_2 = 3\ \text{Cryolite} + 21\ \text{Quartz} + 2\ \text{Magnetite} + 5\ O_2. \quad (23)$$

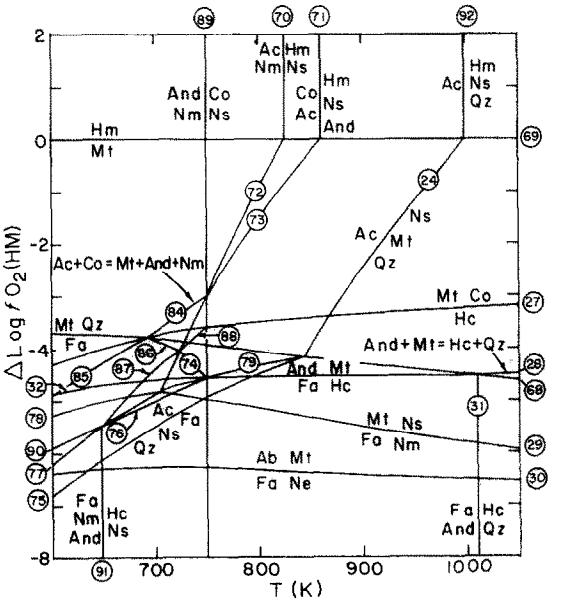

FIG. 6. Reactions independent of fF_2 in the iron-bearing system plotted as a function of $\Delta \log fO_2$ relative to the hematite/magnetite buffer and temperature. Calculations are for 1 bar pressure.

However, reaction (23) is metastable with respect to the reactions limiting the stability of acmite (Fig. 6). Reaction (22) is invariant at fixed pressure and temperature, and metastable with respect to the hematite/magnetite buffer. Acmite is reduced by the reaction

12 Acmite = 6 Natrosilite + 4 Magnetite

$$+ 12 \text{ Quartz} + O_2. \quad (24)$$

This result is somewhat surprising in light of the experiments of ERNST (1962) in which acmite is inferred to be a stable phase at fO_2 conditions below the QFM buffer at approximately 750°C. The experimental error in the calorimetric data for acmite (BENNINGTON, 1981; ±3.0 kJ/mol) is too small to account for this discrepancy. Figure 6 shows the lower stability of acmite as a function of temperature plotted relative to the hematite/magnetite buffer (*cf.* ANOVITZ *et al.*, 1985). Our calculations show that acmite is stable to fO_2 conditions below the QFM buffer only for $T < 570$°C. Reaction (23), which involves natrosilite, is not likely to control the stability of acmite in nature. However, it does represent an absolute limit to acmite stability and suggests that the experimentally derived equilibria of ERNST (1962) are metastable or contain unreported solid-solutions. Reaction (25)

4 Acmite + 3 Nepheline

$$= 3 \text{ Albite} + 2 \text{ Hematite} + 2 \text{ Na-metasilicate} \quad (25)$$

places an upper temperature limit on natural samples with the assemblage pyroxene + nepheline assuming that the effects of pressure and solid-solutions are taken into account (Fig. 7).

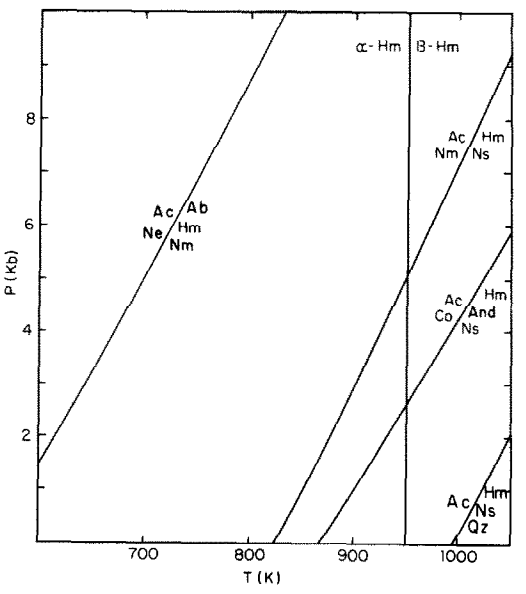

FIG. 7. Reactions limiting the stability of acmite which are independent of both oxygen and fluorine fugacity shown as a function of pressure and temperature.

The phase relations involving fayalite and the iron oxides at lower oxygen fugacities are complex (Fig. 1), but the reactions are symmetrical about the wüstite field. Individual reactions involving iron-bearing phases are related above and below this field by reaction (26):

$$\text{Magnetite} = 3 \text{ Fe} + 2 O_2. \quad (26)$$

Thus, discussions for magnetite-bearing reactions apply equally well for reactions in the iron field, and the iron-bearing reactions are not further discussed.

In the absence of quartz, the presence of corundum, andalusite, natrosilite, or albite severely restricts the stability of magnetite at 1 bar, 1000 K by the reactions:

$$2 \text{ Magnetite} + 6 \text{ Corundum} = 6 \text{ Hercynite} + O_2, \quad (27)$$

2 Magnetite + 6 Andalusite

$$= 6 \text{ Hercynite} + 6 \text{ Quartz} + O_2, \quad (28)$$

2 Magnetite + 3 Natrosilite

$$= 3 \text{ Fayalite} + \text{Na-metasilicate} + O_2, \quad (29)$$

and

4 Magnetite + 3 Albite

$$= 6 \text{ Fayalite} + 3 \text{ Nepheline} + 2 O_2. \quad (30)$$

Reaction (30) restricts the stability of fayalite-nepheline to conditions below the QFM buffer in quartz-undersaturated rocks (Figs. 1, 6). While marked, the effect of temperature on reactions (27)–(30) is similar to that for the QFM buffer (Fig. 6). With the exception of reaction (28), the only changes in these reactions result from their intersections with reactions involving acmite. At 955 K, 1 bar, reaction (28) intersects

2 Hercynite + 3 Quartz

$$= \text{Fayalite} + 2 \text{ Andalusite}. \quad (31)$$

At temperatures below this invariant point the reaction

2 Magnetite + 2 Andalusite

$$= 2 \text{ Fayalite} + 2 \text{ Hercynite} + O_2 \quad (32)$$

limits the lower stability of andalusite + magnetite. While these reactions are metastable with respect to others involving anhydrous Fe-cordierite, calculations of the stable equilibria cannot be conducted until accurate data are available for iron-cordierite.

Reactions in the system Na-Fe-Al-Si-O-F are important for limiting the conditions of formation of many rocks. Below QFM the stabilities of both albite and nepheline are limited in the presence of iron-bearing phases to fluorine fugacities several orders of magnitude below those at which these phases break down at higher oxygen fugacities. For instance, in the presence of magnetite, the stability of albite is limited by reaction (30) in the fluorine-free system, and reactions (58), (61), and (63) in the fluorine/oxygen system at fluorine fugacities well below those defined by reaction

(9). Similarly, the stabilities of chiolite, fluortopaz, and cryolite are limited to more fluorine-rich conditions at oxygen fugacities below QFM than in the iron-free system.

APPLICATIONS

Phase relations in the system Na-Fe-Al-Si-O-F may be used to constrain the P, T, $\log fO_2$, and $\log fF_2$ conditions in a number of metamorphic and igneous environments. These include metamorphosed nepheline syenites, saturated and undersaturated alkaline intrusives (this paper), fayalite granites (BOHLEN and ESSENE, 1978) and topaz rhyolites (BURT, 1979). Calculations in this system may also constrain the fluorine fugacities of any rock in which a mineral or assemblage in the fluorine-free system (*e.g.*, sillimanite or andalusite) is stable at the expense of its fluorine counterpart (*e.g.*, fluortopaz).

We will use the phase equilibria presented above to discuss two examples, the Ivigtut cryolite deposit and the Ilimaussaq alkaline intrusive complex of southwestern Greenland. All analyses referenced in this discussion are listed in Table 11. The Ivigtut body and the Ilimaussaq alkaline intrusion form part of the 1.1 to 1.3 Ga. Gardar intrusive series of southern Greenland (UPTON, 1974). At Ivigtut, the cryolite ore caps a narrow alkaline granite intrusion and is itself capped by a chilled porphyritic microgranitic roof which may have helped to trap the fluorine (BAILEY, 1980). Descriptions of the geology of this body are given by BALDAUF (1910), BØGGILD (1953), PAULY (1960, 1974), BERTHELSEN (1962), BERTHELSEN and HENRIKSEN (1975), BLAXLAND (1976), and BAILEY (1980). The cryolite ore body consisted of several "shells" of differing mineralogy. The main ore body was the siderite-cryolite shell which also contained a few percent quartz, sphalerite, galena, chalcopyrite, pyrite, pyrrhotite, and fluorite. In addition, PAULY (1960) lists nineteen other minerals which have been identified in this unit.

Underlying the siderite-cryolite shell to the west was the fluorite-cryolite shell which also contained topaz, muscovite, weberite, jarlite and chiolite. This was in turn underlain by a shell consisting of fluorite, topaz, muscovite, and quartz. To the east a shell consisting of siderite and quartz underlay the siderite-cryolite ore.

Assuming that the minerals listed above represent equilibrium assemblages, limits may be placed on the $\log (fF_2/fO_2^{0.5})$ conditions of the cryolite deposition in several of the shells. The assemblage cryolite-quartz constrains the siderite-cryolite shell to $\log fF_2/fO_2^{0.5}$ conditions above the reaction

$$\text{Cryolite} + 3\ \text{Quartz} + O_2 = 2\ \text{Villiaumite} + \text{Albite} + 2\ F_2 \quad (33)$$

and below the volatilization of quartz (reaction 18). The assemblage cryolite-topaz-chiolite restricts the $\log (fF_2/fO_2^{0.5})$ conditions of the fluorite-cryolite shell by the breakdown of chiolite to cryolite and corundum:

$$3\ \text{Chiolite} + 3\ O_2 = 5\ \text{Cryolite} + 2\ \text{Corundum} + 6\ F_2 \quad (34)$$

and by reaction (10), which involves the fluoridation of cryolite and topaz to chiolite and quartz. At 1000 K reactions (10) and (33) restrict $\Delta \log (fF_2/fO_2^{0.5})$ in the fluorite-cryolite shell to within 0.55 log units (Fig. 1).

The Ilimaussaq intrusion represents a series of rocks crystallized from a highly undersaturated peralkaline magma. LARSEN (1976) considered that most, if not all of the rock layers present formed as cumulates. Two layers within this body, sodalite foyalite and naujaite contain apatite, magnetite, fayalite, hedenbergite, alkali feldspar, nepheline, sodalite and eudialyte, which Larsen considered to be a liquidus (approximately 800°C) assemblage. Aegirine also appears in these rocks as an intercumulous phase which is interpreted to have formed at or near the solidus at approximately 500°C (LARSEN, 1976). In addition, BONDAM and FERGUSON (1962) reported the occurrence of villiaumite in the

Table 11. Mineral Formulae from the Ilimaussaq Intrusion, Greenland.

Rock	Naujaite							Sodalite Foyalite					
Mineral*	Oliv	Mt	Ksp	Ne	Hd	Ac	Vl	Oliv	Mt	Ksp	Ne	Hd	Ac
Si_{IV}	1.00	--	3.00	0.99	1.95	1.98	--	1.00	--	3.00	0.99	1.95	1.98
Al_{IV}	--	--	0.99	1.00	0.04	0.02	--	--	--	0.99	1.00	0.04	0.02
Al_{VI}	--	--	--	--	--	0.02	--	--	--	--	--	--	0.02
Ti	--	0.65	--	--	0.02	0.00	--	--	0.65	--	--	0.01	0.04
Zr	--	--	--	--	0.01	--	--	--	--	--	--	0.00	--
Fe^{3+}	--	0.70	0.01	0.01	0.14	0.97	--	--	0.70	0.01	0.01	0.11	0.84
Fe^{2+}	1.91	1.65	--	--	0.82	--	--	1.89	1.65	--	--	0.84	0.07
Mn	0.07	--	--	--	0.03	0.00	--	0.08	--	--	--	0.03	0.01
Mg	0.00	--	--	0.00	0.02	--	--	0.01	--	--	0.00	0.04	--
Ca	0.02	--	--	0.01	0.85	0.01	--	0.02	--	--	--	0.90	0.10
Na	--	--	0.31	0.74	0.14	0.99	1.00	--	--	0.31	0.74	0.08	0.93
K	--	--	0.69	0.25	--	--	--	--	--	0.69	0.25	--	--
F	--	--	--	--	--	--	1.00	--	--	--	--	--	--
O	4.00	3.00	8.00	4.00	6.00	6.00	--	4.00	3.00	8.00	4.00	6.00	6.00

* Olivine, magnetite and pyroxene analyses from Larsen (1976), feldspar and nepheline from Currie et al. (1975), villiaumite analysis from Bondam and Ferguson (1962).

naujaite, although it is unclear whether it formed as part of the crystallization sequence or during a later subsolidus event.

The assemblage feldspar-magnetite-fayalite-nepheline fixes fO_2 by reaction (30). At 1000 K, 1 bar the calculated $\log fO_2$ values for the sodalite foyalite and the naujaite are -19.2 and -19.3, respectively, when corrected for solid-solutions using the models of SPENCER and LINDSLEY (1981) for magnetite, and NEWTON *et al.* (1980) for albite, and assuming ideal mixing for nepheline and fayalite.

The QFM buffer allows additional constraints to be placed on the conditions of crystallization of the Ilimaussaq intrusion. LARSEN (1976) noted that given the absence of quartz and the presence of magnetite and fayalite, oxygen fugacities at Ilimaussaq were probably reduced well below QFM. This analysis is supported by our calculations which place the fugacity of oxygen approximately 3.2 log units below QFM at 1000 K. As fO_2 is known from reaction (29), however, calculation of the QFM buffer may be used to find the activity of SiO_2 in these rocks. For the average fO_2 this calculation yields $\log_{10} aSiO_2 = -1.1$. If we assume that the reported villiaumite equilibrated with albite and nepheline, limits may be placed on the fF_2 in the naujaite. The assemblage nepheline-villiaumite limits the maximum fF_2 by reaction (6), while reaction (35)

$$\text{Nepheline} + 2\ \text{Na-metasilicate} + 2\ F_2 = \text{Albite} + 4\ \text{Villiaumite} + O_2 \quad (35)$$

allows calculation of a minimum fluorine fugacity for the assemblage albite-villiaumite. Using the average fO_2 calculated above, $-33.0 \leq \log fF_2 \leq -31.8$ at 1000 K.

Fluorine fugacities are important sensors of the local environments in a wide variety of alkaline rocks. The mineral assemblages found in the system Na-Fe-Al-Si-O-F will define or constrain fO_2, fF_2 and temperature in other alkalic intrusives, metapelites, and A-type granites. These reactions may also be useful for limiting fluorine and oxygen fugacities in rocks which contain no fluorine-bearing phases. In addition, the thermodynamic data and the phase equilibria derived from them serve as a basis from which reactions in more complex systems (*e.g.*, Na-K-Ca-Fe-Al-Si-O-F-H) may be calculated.

Acknowledgements—Work on this project was supported by NSF grants EAR-80-09538 and EAR-84-08168 to E. J. Essene. We would like to thank Dr. D. R. Peacor for allowing us to use his unpublished data on the thermal expansion of cryolite. Reviews by M. D. Barton, D. M. Burt, E. H. Christianson, J. H. Haas Jr., J. M. Ferry and G. R. Robinson Jr. were of great help in preparing this manuscript.

Editorial handling: J. M. Ferry

REFERENCES

ALBRIGHT D. M. (1956) The high temperature thermodynamic properties of cryolite. Ph.D. dissertation, Carnegie-Mellon Univ.

ANOVITZ L. M. and ESSENE E. J. (1987) Compatibility of geobarometers in the system CaO-FeO-Al_2O_3-SiO_2-TiO_2 (CFAST): implications for garnet mixing models. *J. Geol.* (in press).

ANOVITZ L. M., TREIMAN A. H., ESSENE E. J., HEMINGWAY B. S., WALL V. J., WESTRUM E. F. JR., BURRIEL R. and BOHLEN S. R. (1985) The heat capacity of ilmenite and phase equilibria in the system Fe-Ti-O. *Geochim. Cosmochim. Acta* **49**, 2027–2040.

ANOVITZ L. M., ESSENE E. J. and PERKINS D. III (1987) Further calculations in the system Al_2O_3-SiO_2-H_2O. *Clays Clay Minerals* (in preparation).

BAILEY J. C. (1980) Formation of cryolite and other aluminofluorides: A petrologic review. *Bull. Geol. Soc. Denmark* **29**, 1–45.

BALDAUF R. (1910) Uber das Kryolith-Vorkommen in Grønland. *Z. Prakt. Geol.* **18**, 11–12.

BARTON M. D. (1982) The thermodynamic properties of topaz solid solutions and some petrologic applications. *Amer. Mineral.* **67**, 956–974.

BARTON M. D., HASELTON H. T. JR., HEMINGWAY B. S., KLEPPA O. J. and ROBIE R. A. (1982) The thermodynamic properties of fluor-topaz. *Amer. Mineral.* **67**, 350–355.

BENNINGTON K. O. (1981) Some techniques and measurements with HF solution calorimetry. In *Proceedings of the Workshop on Techniques for Measurement of Thermodynamic Properties* (eds. N. A. GOKCEN, R. V. MRAZEK and L. B. PANKRATZ). *U.S. Bur. Mines Info. Circ.* 8853, 173–178.

BERTHELSEN A. (1962) On the geology of the country around Ivigtut, SW-Greenland. *Geol. Rundsch.* **52**, 269–280.

BERTHELSEN A. and HENRIKSEN N. (1975) Geological map of Greenland 1:100,000. Ivigtut 61 V. I Syd. The orogenic and cratonic geology of a Precambrian shield area. *Medd. Grønl.* **186**.

BLAXLAND A. B. (1976) Rb-Sr isotopic evidence for the age and origin of the Ivigtut granite and associated cryolite body, South Greenland. *Econ. Geol.* **71**, 864–869.

BØGGILD O. B. (1953) The mineralogy of Greenland. *Medd. Grønl.* **149**, 1–442.

BOHLEN S. R. and ESSENE E. J. (1978) The significance of metamorphic fluorite in the Adirondacks. *Geochim. Cosmochim. Acta* **42**, 1169–78.

BOHLEN S. R., DOLLASE W. A. and WALL V. J. (1986) Calibration and applications of spinel equilibria in the system FeO-Al_2O_3-SiO_2. *J. Petrol.* **27**, 1143–1156.

BONDAM J. and FERGUSON J. (1962) An occurrence of villiaumite in the Ilimaussaq intrusion, South Greenland. *Medd. Grønl.* **172**, 1–13.

BRYNESTAD J., GRJOTHEIM K. and URNES S. (1960) Interpretation of molten cryolite and of cryolite melts containing Al_2O_3. *Metalurgia Italiana* **52**, 495–502.

BROSSET C. (1938) The crystal structure of chiolite. *Z. Anorg. Allgem. Chem.* **238**, 201–208.

BURT D. M. (1972) The influence of fluorine on the facies of Ca-Fe-Si skarns. *Carnegie Inst. Wash. Yearb.* **71**, 185–197.

BURT D. M. (1979) Geometrical analysis of cryolite and related mineral stabilities in the system Na_2O-Al_2O_3-SiO_2-F_2O_{-1}. *Eos* **60**, 965.

BURT D. M. and LONDON D. (1982) Subsolidus Equilibria. In *Granitic Pegmatites in Science and Industry, MAC Short Course Handbook* (ed. P. CERNY), Vol. 8, pp. 329–346.

CHASE M. W. JR., DAVIES C. A., DOWNEY J. R. JR., FRURIP D. J., MCDONALD R. A. and SYVERUD A. N. (1985) JANAF Thermochemical Tables, Third Edition. *J. Phys. Chem. Ref. Data* **14**, Supp. 1.

CLARK S. P., JR. (1959) Effect of pressure on the melting points of eight alkali halides. *J. Chem. Phys.* **31**, 1526–1531.

CLAUSEN V. H. (1936) Pulver- und Drehphotogramme von Chiolith. *Z. Kryst.* **95**, 394–403.

CODATA (1977) Recommended key values for thermodynamics. *CODATA Bull.* **28.**

CURRIE K. L., CURTIS L. W. and GITTENS J. (1975) Petrology of the Red Wine alkalic complexes, central Labrador and a comparison with the Ilimaussaq complex, southwest Greenland. *Geol. Surv. Can. Pap.* **75,** 271–280.

DEWING E. W. (1970) Thermodynamics of the system NaF-AlF_3. Part II: The free energies of formation of chiolite ($Na_5Al_3F_{14}$). *Met. Trans.* **1,** 2211–2215.

DOUGLAS T. B. and DITMARS D. A. (1967) Measured relative enthalpy of anhydrous crystalline aluminum trifluoride, AlF_3, from 273 to 1173°K and derived thermodynamic properties from 273 to 1600°K. *J. Res. Nat. Bur. Standards* **71,** 185–193.

EBERT F. (1931) The crystal structure of some fluorides of the eighth group of the periodic system. *Z. Anorg. Chem.* **196,** 395–402.

ERNST W. G. (1962) Synthesis, stability relations, and occurrence of riebeckite and riebeckite-arfvedsonite solid solutions. *J. Geol.* **70,** 689–736.

FRANK W. B. (1961) Thermodynamic considerations in the aluminum-producing electrolyte. *J. Phys. Chem.* **65,** 2081–2087.

GRUND A. and PIZY M. (1952) Crystal structure of anhydrous sodium metasilicate. *Acta Cryst.* **5,** 837–840.

HAAS J. L. JR. and FISHER J. R. (1976). Simultaneous evaluation and correlation of thermodynamic data. *Amer. J. Sci.* **276,** 525–545.

HASELTON H. T. JR., HOVIS G. L., HEMINGWAY B. S. and ROBIE R. A. (1983) Calorimetric investigation of the excess entropy of mixing in analbite-sanidine solid solutions: lack of evidence for Na,K short-range order and implications for two-feldspar thermometry. *Amer. Mineral.* **68,** 398–413.

HEMINGWAY B., KRUPKA K. M. and ROBIE R. A. (1981) Heat capacities of the alkali feldspars between 350 and 1000 K from differential scanning calorimetry; the thermodynamic functions of the alkali feldspars from 298.15 to 1400 K, and the reaction quartz + jadeite = analbite. *Amer. Mineral.* **66,** 1205–1215.

HEMINGWAY B. S., ROBIE R. A., KITTRICK J. A., GREW E. S., NELEN J. A. and LONDON D. (1984) The thermodynamic properties of two natural chlorites to 500 K, the heat capacities of osumilite from 298.15 to 1000 K, and the thermodynamic properties of petalite to 1800 K. *Amer. Mineral.* **69,** 701–710.

HOLM B. J. and GRØNVOLD F. (1973) Enthalpies of fusion of the alkali cryolites determined by drop calorimetry. *Acta Chim. Scand.* **27,** 2043–2050.

JOINT COMMITTEE ON POWDER DIFFRACTION STANDARDS (1968) *Set 18 of the Powder Diffraction File* (ed. L. G. BERRY). Philadelphia.

KELLEY K. K. (1960) Contributions to the data on theoretical metallurgy. XI: High-temperature heat-content, heat capacity, and entropy data for the elements and inorganic compounds. *U.S. Bur. Mines. Bull.* **584.**

KELLEY K. K., NAYLOR B. F. and SHOMATE C. H. (1946) The thermodynamic properties of manganese. *U.S. Bur. Mines. Tech. Pap.* **686.**

KING E. G. (1957) Low temperature heat capacities and entropies at 298.15°K of cryolite, anhydrous aluminum fluoride and sodium flouride. *J. Amer. Chem. Soc.* **79,** 2056–2057.

KO H. C., STUVE J. M. and FERRANTE M. J. (1977) Thermophysical properties of acmite. *7th Symposium on Thermophysical Properties,* 392–395.

KOGARKO L. N. (1966) Physical-chemical analysis of cryolite parageneses. *Geokhim.* **2,** 1300–1310.

LACROIX A. (1908) Sur l'existence du fluorine de sodium cristallisé comme élément des syénites néphéliniques des îles de Los. *C. R. Acad. Sci.* (Paris) **196,** 213–216.

LANDON G. J. and UBBELOHDE A. R. (1957) Melting and crystal structure of cryolite (3NaF, AlF_3). *R. Soc. London Proc.* **240,** 160–172.

LARSEN L. M. (1976) Clinopyroxenes and coexisting mafic minerals from the alkalic Ilimaussaq intrusion, South Greenland. *J. Petrol.* **17,** 258–290.

MAJUMDAR A. J. and ROY R. (1965) Test of the applicability of the Clapeyron relation of a few cases of solid-solid transitions. *J. Inorg. Nuc. Chem.* **27,** 1961–1973.

MCADIE H. G., GARN P. D. and MENIS O. (1972) Standard reference materials: Selection of differential thermal analysis temperature standards through a cooperative study (SRM 758, 759, 760). *U.S. Nat. Bur. Standards Spec. Pub.* **260,** 40.

METZ G. W., ANOVITZ L. M., ESSENE E. J., BOHLEN S. R., WESTRUM E. F. JR. and WALL V. J. (1983) Heat capacity from 8 to 1000 K and phase equilibria of almandine. *Eos* **64,** 346–347.

NEWTON R. C., CHARLU T. V. and KLEPPA O. J. (1980) Thermochemistry of the high structure state plagioclases. *Geochim. Cosmochim. Acta* **44,** 933–941.

O'BRIEN C. J. and KELLEY K. K. (1957) High temperature heat contents of cryolite, anhydrous aluminum fluoride and sodium fluoride. *J. Amer. Chem. Soc.* **79,** 5616–5618.

PAULY H. (1960) Paragenetic relations in the main cryolite ore of Ivigtut, South Greenland. *N. Jb. Mineral. Abh.* **94.**

PAULY H. (1974) Ivigtut cryolite deposit, southwest Greenland. In *Metallization Associated with Acid Magmatism* (ed. M. STEMPROK), Vol. 1, 393–399. *Geol. Surv. Czechoslovakia.*

PHILLIPS N. W. F., SINGLETON R. H. and HOLLINGSHEAD E. A. (1955a) Liquidus curves for Al cell electrolyte (I) cryolite-Al_2O_3. *J. Electrochem. Soc.* **102,** 648–649.

PHILLIPS N. W. F., SINGLETON R. H. and HOLLINGSHEAD E. A. (1955b) Liquidus curves for Al cell electrolyte (II) ternary systems of cryolite-Al_2O_3 with NaF, NaCl and AlF_3. *J. Electrochem. Soc.* **102,** 690–692.

RICHET P., BOTTINGA Y., DENIELOU L., PETITET J. P. and TEQUI C. (1982) Thermodynamic properties of quartz, cristobalite and amorphous SiO_2: drop calorimetry measurements between 1000 and 1800 K and a review from 0 to 2000 K. *Geochim. Cosmochim. Acta* **46,** 2639–2658.

ROBIE R. A. and HEMINGWAY B. S. (1972) Calorimeters for heat of solution and low-temperature heat capacity measurements. *U.S. Geol. Surv. Prof. Pap.* **755,** 32p.

ROBIE R. A. and HEMINGWAY B. S. (1984) Entropies of kyanite, andalusite, and sillimanite: additional constraints on the pressure and temperature of the aluminosilicate triple point. *Amer. Mineral.* **69,** 298–306.

ROBIE R. A., HEMINGWAY B. S. and WILSON W. H. (1976) The heat-capacities of Calorimetric Conference copper and of muscovite ($KAl_2(AlSi_3)O_{10}(OH)_2$), pyrophyllite ($Al_2Si_4O_{10}(OH)_2$), and illite ($K_3(Al_7Mg)(Si_{14}Al_2)O_{40}(OH)_8$) between 15 and 375 K and their standard entropies at 298.15 K. *J. Res. U.S. Geol. Surv.* **4,** 631–644.

ROBIE R. A., HEMINGWAY B. S. and FISHER J. P. (1979) Thermodynamic properties of minerals and related substances at 298.15K (25°C) and one bar (10^5 pascals) pressure and at a higher temperatures (revised 1979). *U.S. Geol. Surv. Bull.* **1452,** 456p. (originally printed in 1978).

ROBIE R. A., FINCH C. B. and HEMINGWAY B. S. (1982) Heat capacity between 5.1 and 383 Kelvin and entropy of fayalite (Fe_2SiO_4): Comparison of calorimetric and equilibrium values for the QFM buffer reaction. *Amer. Mineral.* **67,** 463–469.

ROBINSON G. R. JR., HAAS J. L. JR., SCHAFER C. M. and HASELTON H. T. JR. (1982) Thermodynamic and thermophysical properties of selected phases in the MgO-SO_2-H_2O-CO_2, CaO-Al_2O_3-SO_2-H_2O-CO_2, and Fe-FeO-Fe_2O_3-SO_2 chemical systems, with special emphasis on the properties of basalts and their mineral components. *U.S. Geol. Surv. Open-File Rept.*, 83–79.

ROLIN M. (1952) Cryoscopy in fused cryolite and ionic con-

stitution of dissolved aluminum. *Bull. Soc. Francaise Electricieus* **2**, 35–56.

ROLIN M. (1960) Sur la structure ionique de la cryloithe pure fondue. IV. Compatibilité du schema $AlF_6 = AlF_4 + 2F_2$ avec le diagramme experimental. *Bull. Soc. Chim. France*, 681–685.

ROTH W. A. and BERTRAM W. (1979) Messung des Spezifischen Warmen von Metallurgisch Wichtigenstoffen in einem Grosseren Temperaturintervall mit Hilfe von Zwei Neuen Calorimetertypen. *Z. Electrochemie* **35**, 297–308.

SKINNER B. J. (1966) Thermal expansion. In *Handbook of Physical Constants* (ed. S. P. CLARK). *Geol. Soc. Amer. Mem.* **97**, 75–96.

SPENCER K. J. and LINDSLEY D. H. (1981) A solution model for coexisting iron-titanium oxides. *Amer. Mineral.* **66**, 1189–1201.

STEWARD E. G. and ROOKSBY H. P. (1953) Transitions in crystal structure of cryolite and related fluorides. *Acta Cryst.* **6**, 49–52.

STORMER J. C. JR. and CARMICHAEL I. S. E. (1970) Villiaumite and the occurrence of fluoride minerals in igneous rocks. *Amer. Mineral.* **55**, 126–134.

STUVE J. M. and FERRANTE M. J. (1980) Low-temperature heat capacities and high-temperature enthalpies of chiolite ($Na_5Al_3F_{14}$). *U.S. Bur. Mines. Rept. Invest.* 8442.

STULL D. R. and PROPHET H. (1971) JANAF Thermochemical Tables. National Standard Reference Series, *U.S. Nat. Bur. Standards.* **37**.

TIMOSHENKOV I. M., MENSHIKOV YU. P., GANNIBAL L. F. and BUSSEN I. V. (1975) A natural sodium silicate, natrosilite, from the Lovozero massif. *Zap. Vses. Mineral. Obshch.* **104**, 317–321.

UPTON B. G. J. (1974) The alkaline province of Southwest Greenland. In *The Alkalic Rocks* (ed. H. SORENSEN), pp. 221–238. John Wiley.

VLASOV K. A., KUZ'MENKO M. Z. and ES'KOVA E. M. (1966) *The Lovozero Alkali Massif* (Engl. trans.). Hafner Pub. Co., New York.

WESTRUM E. F. JR. (1984) Computerized adiabatic thermophysical calorimetry. In *Proceedings NATO Advanced Study Institute on Thermochemistry at Viana de Castello, Portugal* (ed. M. A. V. RIBERIO DA SILVA), pp. 745–776.

WESTRUM E. F. JR., FURUKAWA G. T. and MCCULLOUGH J. P. (1968) Adiabatic low-temperature calorimetry. In *Experimental Thermodynamics* (ed. J. P. MCCULLOUGH and D. W. SCOTT), Vol. 1, pp. 133–214. Butterworths and Co.